A Kinetic Evaluation of Carbon−Hydrogen, Carbon−Carbon, and Carbon−Silicon Bond Activation in Benzylic Radical Cations

Mauro Freccero,*,†,§ Albert Pratt,*,† Angelo Albini,‡ and Conor Long†

Contribution from the School of Chemical Sciences, Dublin City University, Dublin 9, Ireland, and Dipartimento di Chimica Organica dell'Università di Pavia, viale Taramelli 10, 27100 Pavia, Italy

Received March 24, 1997

Abstract: A detailed study of the competition between C−C, C−H, and C−Si bond fragmentation in a series of 4-methoxy-α-substituted toluene radical cations (**1**$^{\bullet+}$), involving both product studies and kinetic analysis, is presented. C−C bond fragmentation occurs with several radical cations in acetonitrile. The rate constants for such processes, determined by laser flash photolysis, varied from 2.8×10^4 (**1c**$^{\bullet+}$) to 1.53×10^6 (**1f**$^{\bullet+}$) s^{-1}. The activation parameters for C−C bond fragmentation are characterized by low activation enthalpies on the order of 30 kJ mol^{-1} and negative activation entropies in the range −34 to −55 J mol^{-1} K^{-1}. Deprotonation of the radical cations is always a second-order process induced by nucleophiles [cerium(IV) ammonium nitrate (CAN) or nitrate anion], with second-order rate constants from 7.7×10^7 (**1h**$^{\bullet+}$) to 8.8×10^8 (**1i**$^{\bullet+}$) M^{-1} s^{-1} in neat acetonitrile (CAN assisted) and from 0.4×10^8 (**1j**$^{\bullet+}$) to 7.1×10^8 (**1i**$^{\bullet+}$) M^{-1} s^{-1} in the presence of nitrate anion. The rate constant for nitrate-induced decarboxylation was higher, 13.6×10^8 M^{-1} s^{-1} (**1d**$^{\bullet+}$). In a few cases C−C (**1e**$^{\bullet+}$, **1f**$^{\bullet+}$) and C−Si (**1g**$^{\bullet+}$) fragmentations occurred, also as second-order processes induced by nitrate, with rate constants from 4.4×10^8 (**1f**$^{\bullet+}$) to 8.2×10^8 (**1g**$^{\bullet+}$) M^{-1} s^{-1}. $\Delta H^{\ddagger}$ and $\Delta S^{\ddagger}$ had opposing influences on C−H and C−C fragmentation, and in the case of **1e**$^{\bullet+}$ a temperature-dependent product distribution was obtained. The activation parameters for the observed C−H, C−C, and C−Si fragmentations have been compared, and suggest a rationale for the mechanisms and selectivity of such processes in radical cations.

Introduction

Ion radicals play a key role in redox reactions involving organic substrates,[1] and interest in their reactivity continues to grow. Removal of an electron from a neutral molecule often results in bond weakening within the resulting radical cation. This process increases the rate of heterolytic fragmentation and has been proven to be a useful method for the generation of radicals for synthetic purposes.[1b,e−i,m] The most common reaction of cation radical intermediates is α-heterolytic fragmentation with loss, or transfer to the solvent or to a nucleophile, of an electrofugal group (X^+), as shown in Scheme 1. Arene

Scheme 1

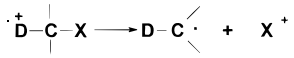

cation radical α-deprotonation,[2,3] desilylation,[4,5] and decarboxylation[6] are the most common fragmentations of this type. Most studies in this area have been devoted to deprotonation and are based on product distribution analysis,[2,4,6a] or the measurement of absolute rates[3,6d,7,8] and their response to variations in base strength[7−9] or to steric and electronic effects.[2,9−11] Recent investigations of α-trialkylsilyl-substituted cation radical desilylations have shown that these processes are dependent on the nature of the silicon substituent[5] and on the medium charac-

† Dublin City University.
‡ Università di Pavia.
§ Current address: Università di Pavia.

(1) (a) *Electron-Transfer Reactions in Organic Chemistry*; Eberson L., Ed.; Springer: Berlin, Heidelberg, New York, 1987; see also references therein cited. (b) *Advances in Electron-Transfer Chemistry*; Mariano, P. S., Ed.; JAI Press: Greenwich, CT, 1991−94; Vols. 1−4. (c) *Top. Curr. Chem.* Mattay, J., Ed.; **1990**−**94**, *156, 158, 159, 163, 168, 169*. (d) *Photoinduced Electron Transfer*; Fox, M. A., Chanon, M., Eds.; Elsevier: Amsterdam, 1988; Parts A, B, and C and references therein. (e) *Photochemical Key Steps in Organic Synthesis;* Mattay, J., Griesbeck, A.; Eds.; VCH: Weinheim, 1994. (f) Chiu, F.-T.; Ullrich, J. W.; Mariano, P. S. *J. Org. Chem.* **1984**, *49*, 228. (g) Albini, A.; Mella, M.; Freccero, M.; *Tetrahedron* **1994**, *50*, 575. (h) Mella, M.; d'Alessandro, N.; Freccero, M.; Albini, A. *J. Chem. Soc., Perkin Trans. 2* **1993**, 515. (i) Fagnoni, M.; Mella, M.; Albini, A. *J. Am. Chem. Soc.* **1995**, *117*, 7877. (j) Albini, A.; Mella, M. *Tetrahedron* **1986**, *42*, 6219. (k) Albini, A.; Fasani, E.; Mella, M. *J. Am. Chem. Soc.* **1986**, *108*, 4119. (l) Mariano, P. S.; Stavinoha, J. L. In *Synthetic Organic Photochemistry;* Horspool, W. M., Ed.; Plenum Press: London, 1984. (m) Yoon, U. C.; Mariano, P. S. *Acc. Chem. Res.* **1992**, *25*, 233. (n) Gaillard, R. E.; Whitten, D. G. *Acc. Chem. Res*. **1996**, *29*, 292. (o) Albini, A.; Siviero, E.; Mella, M.; Long, C.; Pratt, A.; *J. Chem. Soc., Perkin Trans. 2* **1995**, 1895.

(2) Lewis, F. D. *Acc. Chem. Res*. **1986**, *19*, 401.
(3) Schlesener, C. J.; Amatore, C.; Kochi, J. K. *J. Am. Chem. Soc.* **1984**, *106*, 7472.
(4) Ohga, K.; Yoon, U. C.; Mariano, P. S. *J. Org. Chem*. **1984**, *49*, 213.
(5) Dinnocenzo, J. P.; Farid, S.; Goodman, J. L.; Gould, I. R.; Todd, W. R.; Mattes, S. L. *J. Am. Chem. Soc.* **1989**, *111*, 8973.
(6) (a) d'Alessandro, N.; Albini, A.; Mariano, P. S. *J. Org. Chem.* **1993**, *58*, 937. (b) Budac, D.; Wan, P. *J. Photochem. Photobiol., A: Chem.* **1992**, *67*, 135. (c) Meiggs, T. O.; Grossweiner, L. I.; Miller, S. I. *J. Am. Chem. Soc.* **1972**, *94*, 7981. (d) Steenken, S.; Warren, C. J.; Gilbert, B. C. *J. Chem. Soc., Perkin Trans. 2* **1990**, 335. (e) Davidson, R. S.; Steiner, P. R. *J. Chem. Soc., Perkin Trans. 2* **1972**, 1557.
(7) Dinnocenzo, J. P.; Banach, I. E. *J. Am. Chem. Soc*. **1989**, *111*, 8646.
(8) Baciocchi, E.; Del Giacco, T.; Elisei, F. *J. Am. Chem. Soc*, **1993**, *115*, 12290.
(9) Zhang, X.; Yeh, S.-R.; Hong, S.; Freccero, M.; Albini, A.; Falvey, D.; Mariano, P. S. *J. Am. Chem. Soc*. **1994**, *116*, 4211.
(10) Baciocchi, E.; Mattioli, M.; Romano, R.; Ruzziconi, R. *J. Org. Chem.* **1991**, *56*, 7154.
(11) Tolbert, L. M.; Khanna, R. K.; Popp, A. E.; Gelbaum, L.; Bottomley, L. A. *J. Am. Chem. Soc.* **1990**, *112*, 2373.

S0002-7863(97)00940-2 CCC: $15.00
Published on Web 01/06/1998

teristics,[9,12] and that they can compete with or be dominant over cation radical α-deprotonation.[9] Cleavage of C−C bonds in radical cations has attracted considerable attention in the past decade.[13−15] With only a few exceptions,[7,16−19] kinetic data for evaluation of the extent of C−H and C−C bond activation in radical cations have been unavailable.

Mechanisms have frequently been inferred from product studies. Fragmentation reaction selectivities have been generally rationalized through a thermochemical approach by comparing the bond dissociation energies (ΔH) obtained from thermochemical cycles.[1g,h,13−15] This approach has been successful only within a homogeneous series of compounds involving fragmentation of a particular bond type,[13,20] but failed systematically for different competing fragmentation processes. This was particularly true when direct comparison of C−H and C−C bond fragmentations in cation radicals was attempted.[1g,h,20]

We therefore deemed it worthwhile to carry out an extensive kinetic investigation of the fragmentation of different C−X bond types (X = H, C, Si) in arene cation radicals and to determine the activation parameters for these processes. A series of 4-methoxybenzyl derivatives, for which thermochemical evaluation[21] predicted competitive fragmentation processes involving the cation radical, was chosen. In preliminary attempts, the cation radicals were produced by PET (photoinduced electron transfer) to an organic molecule. However, it became apparent at an early stage that a more efficient way to generate such species is by SET (single electron transfer) to the nitrate radical. Our results have identified and rationalized the mode of fragmentation of each cation radical, providing a mechanistic picture of the fragmentation based on the activation parameters of the different processes involved, and offering new insights into the utility of these species.

Product Distribution Analysis

Steady-state photochemical studies were carried out to confirm that irradiation of solutions containing cerium(IV) ammonium nitrate $(NH_4)_2Ce(NO_3)_6$ (CAN**)** and benzylic donors (**1)** gave products consistent with SET and subsequent C−H, C−C, or C−Si bond fragmentations within the radical cations.

Scheme 2

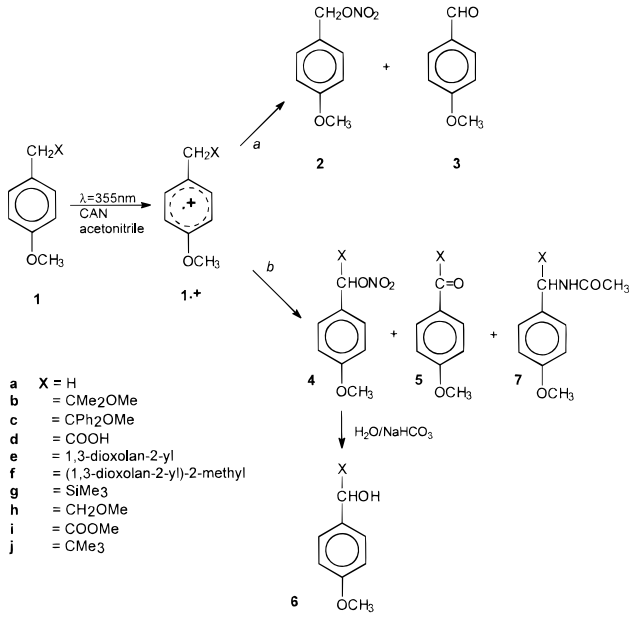

Preparative Irradiations in Neat Acetonitrile. Acetonitrile solutions of the 4-methoxy-α-substituted toluenes **1a**−**g** (10 mM) (Scheme 2, Table 1) were irradiated in the presence of CAN (20 mM), with a 400 W medium-pressure mercury vapor lamp through a Pyrex filter at room temperature. In every case, 4-methoxybenzyl nitrate (**2**) was obtained as the main product, with 4-methoxybenzaldehyde (**3**) as the minor one (Scheme 2, path a). In the case of ethers **1b** and **1c**, acetone and benzophenone, respectively, were formed concurrently with the above compounds. Likewise, 2-hydroxyethyl formate and 2-hydroxyethyl acetate were formed from **1e** and **1f**, respectively. Separate experiments showed that the aldehyde **3** was formed from further irradiation of CAN in the presence of compound **2**.

Similar irradiation of the 4-methoxy-α-substituted toluenes **1h** and **1i** in the presence of CAN led to clean formation of the α-substituted nitrates **4h** and **4i,** respectively, as the major products. Due to its instability, the nitrate **4h** was hydrolyzed and characterized as the alcohol **6h**. A minor photoproduct from **1i** was **5i** (9% yield; Scheme 2, path b). On the other hand, irradiation of **1j** under the same conditions did not lead to significant substrate decomposition. Acetamide **7h** was formed in significant yield as an additional product on irradiation in more dilute solution in acetonitrile (CAN, 1 mM; **1h**, 0.5 mM). On the other hand when substrates **1b**, **1c**, **1f**, and **1g** were irradiated at similar dilutions, no amide products were detected. Table 1 gathers the results from the preparative experiments.

Preparative Irradiations with Nitrate Anion as Nucleophile. Irradiation of a deaerated acetonitrile solution of **1** (1 mM) and CAN (2 mM) in the presence of tetrabutylammonium nitrate (5 mM), under the same conditions as above, again gave nitrate **2**, accompanied by small amounts of 4-methoxybenzaldehyde (**3**), from substrates **1a**, **1d**, **1f**, and **1g**. Investigations with the last two substrates showed that this reaction course did not change in the presence of 10 mM nitrate. Compounds **1h** and **1i** again gave the corresponding nitrates **4h** and **4i**.

In contrast, ether **1b** now gave a different reaction, yielding substituted nitrate **4b** as the main product, with a small amount of **3** and a trace of **2**. Ether **1c** behaved similarly, yielding nitrate **4c** and 2-(4-methoxyphenyl)-1,2-diphenylethanone as the main products, accompanied by minor amounts of ketone **5c** as well

(12) (a) Dockery, K. P.; Dinnocenzo, J. P.; Farid, S.; Goodmann, J. L.; Gould, I. R.; Todd, W. P. *J. Am. Chem. Soc.* **1997**, *119*, 1876. (b) Todd, W. R.; Dinnocenzo, J. P.; Farid, S.; Goodman, J. L.; Gould, I. R. *J. Am. Chem. Soc*. **1991**, *113*, 3601. (c) Dinnocenzo, J. P.; Farid, S.; Goodman, J. L.; Gould, I. R.; Todd, W. P. *Mol. Cryst. Liq. Cryst.* **1991**, *194*, 151.

(13) Arnold, D. R.; Maroulis, A. J. *J. Am. Chem. Soc.* **1976**, *98*, 5931.

(14) (a) Okamoto, A.; Arnold, D. R. *Can. J. Chem.* **1985**, *63*, 2340. (b) Okamoto, A.; Snow, M. S.; Arnold, D. R. *Tetrahedron* **1986**, *42*, 6175.

(15) Popielarz, R.; Arnold, D. R. *J. Am. Chem. Soc.* **1990**, *112*, 3068.

(16) (a) Maslak, P.; Chapman, W. H., Jr.; Vallombroso, T. M., Jr.; Watson, B. A. *J. Am. Chem. Soc*. **1995**, *117*, 12380. (b) Maslak, P. *Top. Curr. Chem.* **1993**, *168*, 143. (c) Maslak, P.; Asel, S. L. *J. Am. Chem. Soc*. **1988**, *110*, 8260. (d) Maslak, P.; Vallombroso, T. M.; Chapman, W. H., Jr.; Narvaez, J. N. *Angew. Chem., Int. Ed. Engl.* **1994**, *33*, 73.

(17) (a) Anne, A.; Hapiout, P.; Moiroux, J.; Neta, P.; Savéant, J. M. *J. Am. Chem. Soc.* **1992**, *114*, 4694. (b) Anne, A.; Fraoua, S.; Moiroux, J.; Savéant, J. M. *J. Am. Chem. Soc.* **1996**, *118*, 3938. (c) Savéant[17b] has concluded that an upper limit to the rate of radical ion cleavage is set by the rate of diffusion of the fragments from the solvent cage. Maslak[16d] and Savéant[17b] have established a log k vs ΔG_0 linear free energy relationship for two series of closely related radical ions undergoing C−C bond fragmentation. Given, however, the relatively limited span of the log k data obtained here for benzylic radical cations $\mathbf{1}^{\bullet+}$, we have not considered it worthwhile to attempt a similar analysis.

(18) Parker, V. D.; Tilset, M. *J. Am. Chem. Soc.* **1991**, *113*, 8778.

(19) (a) Burton, R. D.; Bartberger, M. D.; Zhang, Y.; Eyler, J. R.; Schanze, K. S. *J. Am. Chem. Soc.* **1996**, *118*, 5655. (b) Ci, X.; Kellet, M. A.; Whitten, D. G. *J. Am. Chem. Soc.* **1991**, *113*, 3893. (c) Baciocchi, E.; Bietti, M.; Putignani, L.; Steenken, S. *J. Am. Chem. Soc.* **1996**, *118*, 5952.

(20) Baciocchi, E. *Acta Chem. Scand.* **1990**, *44*, 645.

(21) See Table 8 for details of the thermochemical calculations.

Table 1. Products from Preparative Irradiation of CAN in the Presence of 4-Methoxytoluenes **1a**−**j** and Nitrate **2**

4-methoxytoluenes	irradiation time (min)	recovered starting material (%)	products (yield, %)[b]
1a[a]	30	29	**2** (65), **3** (5)
1b[a]	30	38	**2** (55), **3** (7), MeCOMe (∼50)[c]
1c[a]	30	26	**2** (62), **3** (11), PhCOPh (72)
1d[a]	20		**2** (79), **3** (20)
1e[a]	20	10	**2** (70), **3** (15) $HCO_2CH_2CH_2OH$ (85)
1f[a]	20		**2** (95), **3** (3) $MeCO_2CH_2CH_2OH$ (95)
1g[a]	15		**2** (97), **3** (trace)
1h[a]	75	30	**3** (2), **4h** (65)[d]
1h[e]	20	27	**3**(7), **4h** (40), **6h** (8), **7h** (15)
1i[a]	35	40	**4i** (50), **5i** (9)
1j[a]	75	90	**3** (4)
2[f]	30	60	**3** (34)

[a] Irradiation of an acetonitrile solution of CAN (20 mM) and the 4-methoxytoluene (10 mM). [b] Yield relative to the starting 4-methoxytoluene, measured by ^{1}H NMR after workup. [c] Acetone measured by ^{1}H NMR following photolysis in CD_3CN. [d] Determined as the corresponding alcohol (GC, and ^{1}H NMR after addition of internal standard) after hydrolysis (see the Experimental Section). [e] Irradiation of a much more dilute acetonitrile solution of CAN (1 mM) and **1h** (0.5 mM). Product yields were measured by GC. [f] Irradiation of an acetonitrile solution of CAN (20 mM) and 4-methoxybenzylnitrate (10 mM).

Table 2. Products from Preparative Irradiation of CAN and 4-Methoxytoluenes **1a**−**j** in the Presence of Bu_4NNO_3[a]

4-methoxytoluenes	irradiation time (min)	recovered starting material (%)[b]	products (yield, %)[b]
1a	30	10	**2** (75)**, 3** (10)
1b	30	50	**4b** (30),[c] **3** (5), **2** (1)
1c	60	50	**4c** (20),[c] **5c** (5), **3** (3) **2** (1), 4-AnCHPhCOPh (15), PhCOPh (1)
1d	20		**2** (90), **3** (5)
1e	20[d]	43	**4e** (30),[c] **2** (18), **3** (5) $HCO_2CH_2CH_2OH$ (20)
1e	10[e]	30	**4e** (28),[c] **2** (30), **3** (11) $HCO_2CH_2CH_2OH$ (38)
1e	10[f]	30	**4e** (20),[c] **2** (34), **3** (14) $HCO_2CH_2CH_2OH$ (42)
1f	5	19	**2** (78),[g] **3** (trace)[g]
1g	5	10	**2** (85),[g] **3** (trace)[g]
1h	30	20	**4h** (77),[g] **5** (trace)
1i	30	20	**4i** (65), **5** (15)
1j	120	55	**4j** (45)[h]

[a] Irradiation of an acetonitrile solution of CAN (2 mM) and the 4-methoxytoluene (1 mM) containing Bu_4NNO_3 (5 mM). [b] Relative to the starting material. [c] After hydrolysis, the nitrate esters were determined by GC as the corresponding alcohols. [d] At 5 °C. [e] At 25 °C. [f] At 45 °C. [g] Similar results were obtained on increasing the nitrate concentration to 10 mM. [h] Yield measured by ^{1}H NMR.

as by compounds **2**, **3**, and benzophenone. The chemistry of acetal **1e** was more involved, since the outcome was temperature dependent. Thus, nitrate **4e** was the the main low-temperature product ($T \leq 5$ °C), but became the minor one at higher temperatures ($T > 25$ °C), where **2** predominated. The ratio of the yield of **4e** to the combined yields of **2** and **3** dropped from 1.3 to 0.4 with increasing temperature from 5 to 45 °C (Table 2). In parallel with this the yield of 2-hydroxyethyl formate also increased over the same temperature range. Irradiation of compound **1j**, which in the absence of added nitrate did not react appreciably, yielded **4j** as the only product under these conditions. Nitrates **4b, 4c, 4e,** and **4h** were hydrolyzed to the corresponding alcohols **6b, 6c, 6e,** and **6h,** respectively, for easier characterization.

Laser Flash Photolysis Measurements

Laser flash photolysis measurements were used to investigate the involvement of cation radical intermediates in the previously described reactions and to determine their properties. A Nd:YAG laser (power 2−10 mJ, pulse duration 10 ns, $\lambda_{exc} = 355$ nm) was used for the measurements, and the transient absorptions were measured between 440 and 750 nm. At the low laser pulse powers used it may be assumed that only single quantum processes are involved and that the product distributions are the same as in the preparative experiments.

Efficiency of the SET Process Evaluated by Kinetic Data for Oxidation of the Substrates 1. Initially the cation radicals were produced by a PET process using the well-established 9,10-dicyanoanthracene (DCA)/biphenyl (BP)/O_2 system.[5] However, signal intensities (especially for the substrates with higher oxidation potentials) were too weak for accurate kinetic evaluation. As an alternative, SET from **1** to the nitrate radical was explored. This method produced transient absorption intensities at least 10 times greater. Nitrate radicals were generated by photolysis of CAN (0.15 mM in acetonitrile) at 355 nm, and a kinetic study of the oxidation of the *p*-methoxybenzyl derivatives (**1**) under these conditions was carried out. The rate of disappearance of nitrate radicals at 25 °C was monitored at 635 nm in the presence of a measured excess of the aromatic compounds. Plots of the first-order rate constants vs donor

Scheme 3

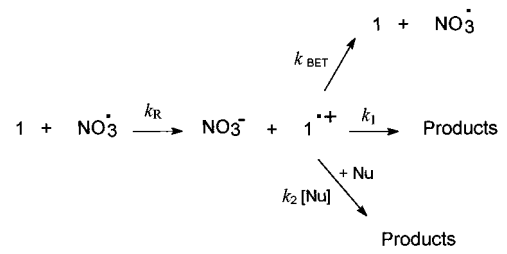

Table 3. Thermochemical and Kinetic Data Relevant to the Oxidative Step (Eq 1) in the Reaction of the Benzylic Donors **1** with Nitrate Radical

4-AnCH$_2$X	E_{ox} (V) (vs SCE)[a]	$-\Delta G$ (eV)[b]	k_R (10^{10} M^{-1} s^{-1})[c]
1a	1.52	0.48	1.38
1b	1.52	0.48	1.12
1c	1.50	0.5	1.03
1d	1.68	0.32	1.10
1e	1.59	0.41	1.14
1f	1.54	0.46	1.35
1g	1.35	0.65	1.14
1h	1.56	0.44	1.25
1i	1.63	0.37	1.11
1j	1.50	0.5	1.35

[a] Oxidation potentials have been estimated from the frequencies of the CT bands in the spectra of mixtures of the benzylic donors **1** and tetracyanoethylene, using the correlation E_o (V vs SCE) = $1068.84\lambda^{-1}$ (nm^{-1}) − 0.371, developed for a series of alkylbenzenes by Kochi,[52] and used by Baciocchi.[8] [b] Calculated using $E°(NO_3^•/NO_3^-) = 2.0$ V vs SCE.[27] [c] Rate constants for reaction of nitrate radical with 4-methoxytoluenes **1a**−**j**, according to the reaction in eq 1.

concentration were linear, and the second-order rate constant for the SET from the benzylic donor to the oxidant radical (k_R, eq 1 and Scheme 3) was calculated from the slope. All the values were diffusion controlled (Table 3).

$$p\text{-AnCH}_2\text{X} + \text{NO}_3^{\bullet} \xrightarrow{k_R} p\text{-AnCH}_2\text{X}^{\bullet+} + \text{NO}_3^- \qquad (1)$$

Evaluation of Nitrate Radical Efficiency in Producing Cation Radicals 1$^{•+}$. The concentration of nitrate radicals formed from CAN (0.15 mM) by a single pulse (laser power 10 mJ) was determined to be [$NO_3^•$] = 1.30×10^{-5} M ($\pm 0.1 \times 10^{-5}$ M) by measuring the end-of-pulse absorbance at 635 nm and using the reported value for the molar absorptivity of this species in acetonitrile [$\epsilon_{NO_3^•}$ (635 nm) = 1300 ± 100 M^{-1} cm^{-1}].[22] When an identical solution containing 10 mM anisole (An) was flashed (using identical laser power), the anisole radical cation was formed and its concentration calculated to be [An$^{•+}$] = 1.26×10^{-5} M ($\pm 0.04 \times 10^{-5}$ M) by measuring the absorbance at 430 nm and using the known $\epsilon_{An^{•+}}$ (430 nm) = 3800 ± 100.[23] The efficiency of formation of the free aromatic cation radicals was 0.97 (±0.03), calculated from the ratio of the anisole cation radical and nitrate radical concentrations. An identical experiment in the presence of 0.8 mM anisole permitted both measurement of the nitrate radical concentration immediately after the pulse and monitoring of the subsequent growth of the anisole cation radical concentration. This reached a maximum value (very similar to that observed in the previous experiment) after 200 ns. Preliminary measurements had shown that oxygen did not affect the kinetics of these species, and subsequent measurements were carried out in air-equilibrated solutions.

Spectroscopic Characterization of the 4-Methoxybenzyl Cation Radicals 1$^{•+}$. After laser excitation of CAN solutions in the presence of compounds **1a**−**j** (5 mM), a rapid decay of nitrate radical absorbance at 635 nm took place (<100 ns) with the concomitant rise of new transients with absorption maxima (λ_{max}) in the 400−650 nm region, similar to the anisole case. These were attributed to the corresponding cation radicals (**1**$^{•+}$) and accorded with previous studies where absorption spectra had been reported for **1a**$^{•+}$ [8,24] and **1g**$^{•+}$.[5,25] In addition, the **1g**$^{•+}$ spectra obtained both in the present work and in the literature[5,12] using the DCA/BP system and that obtained via photoproduced nitrate radical were identical, although for the latter method the signal was much more intense.

The radical cation absorption spectra had features which were dependent on the nature of the α-substituent X (eq 1). In particular, those containing a β-oxygenated function showed either a tail in the spectrum extending to 700 nm (ethers; Figure 1b,c,h), or a second broader band centered close to 540 nm (acetals; Figure 1e,f). Assuming identical efficiencies of formation for the different cation radicals, the molar extinction coefficient for each was determined, the laser power being maintained constant throughout the series of experiments. The results are reported in Table 4, and the corresponding spectra are shown in Figure 1. In all cases the spectra have been corrected between 400 and 440 nm for the depletion of the ground state of CAN.[8] All the transients underwent first-order decay (insets in Figure 1), except for **1j**$^{•+}$, for which it was mainly a second-order process, k_{obs} = 1.5×10^5 M^{-1} s^{-1} (compare this with the lack of reactivity of this substrate in preparative experiments without nitrate; Table 1). The observed decay rate constants (k_{obs}) are reported in Table 4.

Radical Cation Fragmentation. To investigate the cation radical fragmentation mechanisms, the study was extended to include an evaluation of the influence of CAN concentration and of an added nucleophile, the nitrate anion. Rate constants measured for the decay of radical cations **1b**$^{•+}$, **1c**$^{•+}$, **1e**$^{•+}$, **1f**$^{•+}$, and **1g** $^{•+}$ were independent of the laser excitation power (2−10 mJ) and CAN concentration (0.08−0.3 mM) used. For the benzylic donors **1b**, **1c, 1e**, **1f**, and **1g** the kinetics gave an excellent fit in the 420−550 nm range using a first-order decay model. Activation parameters ($\Delta H^‡$ and $\Delta S^‡$) for the bond fragmentations of **1b**$^{•+}$, **1c**$^{•+}$, **1e**$^{•+}$, **1f**$^{•+}$, and **1g**$^{•+}$ were determined from Eyring analysis of k_1 (first-order decay rate constant) over the temperature range 0−40 °C. The excellent linear correlations between ln(k_1/T) and $1/T$ can be seen from the plots in Figure 2. The activation parameters are presented in Table 5a, along with the corresponding radical cation fragmentation process, as deduced from preparative studies (Table 1).

In contrast, the rate constants for decay of radical cations **1a**$^{•+}$, **1d**$^{•+}$, **1h**$^{•+}$, and **1i**$^{•+}$ were a function of CAN concentration. Air-equilibrated acetonitrile solutions of donors **1a**, **1d, 1h**, and **1i** (5 mM) were photolyzed using a laser power of 2 mJ at 355 nm in the presence of CAN at concentrations in the range 0.1−0.3 mM. Under these conditions the radical cation decay rates were pseudo-first-order. Clean first-order decays were found only with laser powers below 10 mJ. At higher intensities the local concentrations of nitrate anion produced during the flash were sufficiently high to compete with CAN (see below). Plots of the pseudo-first-order rate constants vs CAN concentration yielded linear correlations. The second-order rate constants (k_2)

(22) Katsumura, Y.; Jiang, P. Y.; Nagaishi, R.; Oishi, T.; Ishigure, K.; Yoshida, Y. *J. Phys. Chem.* **1991**, *95*, 4435.
(23) O'Neill, P.; Steenken, S.; Schulte-Frohlinde, D. *J. Phys. Chem.* **1975**, *79*, 2773.
(24) Del Giacco, E.; Baciocchi, E.; Steenken, S. *J. Phys. Chem.* **1993**, *97*, 5451.
(25) Cermenati, L.; Freccero, M.; Venturello, P.; Albini, A. *J. Am. Chem. Soc.* **1995**, *117*, 7869.

Table 4. Spectroscopic Characterization of Transients from 4-Methoxytoluenes **1a**−**j**

radical cations $\mathbf{1}^{\bullet+}$	X	k_{obs} (10^4 s^{-1})[a]	absorption range λ (nm)	λ_{max} (nm)	$\epsilon(\lambda_{max})$[b] (M^{-1} cm^{-1})
1a	H	1.0	400−480	430	3800[23]
1b	CMe_2OMe	3.6	400−600	450	3580
1c	CPh_2OMe	2.8	400−690	450	3250
1d	COOH	28.3	400−540	460	3510
1e	1,3-dioxolan-2-yl	8.5	400−700	first, 440	2200
				second, 530	1000[c]
1f	2-methyl-1,3-dioxolan-2-yl	152.8	400−700	first, 440	2200
				second, 550	2500[c]
1g	$SiMe_3$	215.0	400−650	510	5360
1h	CH_2OMe	1.15	400−640	440	3660
1i	COOMe	13.2	400−540	460	3530
1j	CMe_3	*d*	410−530	460	5350

[a] Observed rate constants in acetonitrile (first-order analysis), obtained by flashing the solutions in the presence of CAN (0.15 mM) at 298 K. [b] Extinction coefficients measured at the wavelength of maximum absorption. [c] Measured at 283 K. The molar absorptivity of this part of the spectrum is temperature dependent. [d] In this case a second-order decay, $k_{BET} = 1.5 \times 10^5$ M^{-1} s^{-1}, was observed.

for the cation radical fragmentations induced by CAN were obtained from the slopes of these plots. For cation radicals $\mathbf{1a}^{\bullet+}$, $\mathbf{1d}^{\bullet+}$, $\mathbf{1h}^{\bullet+}$, and $\mathbf{1i}^{\bullet+}$ activation parameters were evaluated from rate constant measurements at several temperatures (8−9 points) in the range 0−40 °C (Table 5b).

Salt Effect on Cation Radical Lifetimes. As part of an examination of the effect of an anionic nucleophile (nitrate anion) on the cation radical lifetimes, the effect of ionic strength on cation radical lifetimes was first investigated by monitoring the lifetime of cation radical $\mathbf{1}^{\bullet+}$ as a function of the concentration of a nonnucleophilic salt (n-Bu_4NClO_4). Acetonitrile solutions of **1a**−**j** (5 mM) were flashed in the presence of CAN and of perchlorate anion in the concentration range 1−10 mM. An effect was noticeable for all cation radicals studied, with the exception of $\mathbf{1f}^{\bullet+}$ and $\mathbf{1g}^{\bullet+}$, the decay of which did not show any salt effect. An increase in cation radical lifetime was observed with $\mathbf{1a}^{\bullet+}$−$\mathbf{1e}^{\bullet+}$, $\mathbf{1h}^{\bullet+}$, and $\mathbf{1i}^{\bullet+}$. The effect was small for $\mathbf{1b}^{\bullet+}$ and $\mathbf{1c}^{\bullet+}$, but it was significant for $\mathbf{1d}^{\bullet+}$ (10%) and reached a maximum for $\mathbf{1a}^{\bullet+}$ (30%; see Figure 3). Thus, although the salt effect was moderate in every case, it did require that the effect of nucleophiles be examined at constant ionic strength to obtain meaningful results.

Cation Radical Fragmentations Induced by an Added Nucleophile. The effect of added nitrate anion on the cation radical lifetimes was studied at constant ionic strength. Acetonitrile solutions of CAN (0.15 mM) and **1a**−**i** (10 mM) were photolyzed at 355 nm (laser power 10 mJ) in the presence of various concentrations of n-Bu_4NNO_3 (1−8 mM), with the ionic strength of the solutions being maintained constant at 8 mM, by appropriate addition of n-Bu_4NClO_4. The decays of the cation radicals followed first-order kinetics under these conditions, and the lifetimes were reduced. A linear correlation was established between the pseudo-first-order rate constants and nitrate anion concentration, and the second-order rate constants (k_2') for nitrate-induced fragmentation were calculated. The activation parameters (for the second-order fragmentation processes) were determined from rate constants measured at several temperatures (over 6−8 points) in the range 0−30 °C, and the calculated $\Delta H^{\ddagger}$ and $\Delta S^{\ddagger}$ values are reported in Table 6.

Discussion

Generation of Cation Radicals. The results presented in Table 3 show that nitrate radical ($NO_3^{\bullet}$) produced by CAN photolysis is an excellent oxidant of the 4-methoxybenzylic substrates **1**. This method[8,26] has been successfully used, mainly by Baciocchi and co-workers, to produce the cation radicals of aromatic substrates.[27,28] Thermochemical and kinetic data (Table 3) suggest that SET according to eq 1 is strongly exergonic and diffusion controlled.

The spectra shown in Figure 1 can be unambiguously attributed to the radical cations $\mathbf{1}^{\bullet+}$. In the case of $\mathbf{1g}^{\bullet+}$, its absorption spectrum, decay rate, and mode of fragmentation (C−Si bond cleavage) are identical whether the cation radical is formed by either the DCA/BP/oxygen method or the CAN method, confirming that in both cases the same solvated species is produced and monitored. In the case of $\mathbf{1a}^{\bullet+}$, the absorption spectrum is also independent of the method used for its generation. However, $\mathbf{1a}^{\bullet+}$ decays much more rapidly when generated by the DCA/BP/oxygen method, perhaps because of the possible presence of $O_2^{\bullet-}$, a stronger base than nitrate anion. The comparative stabilities of similar cation radicals produced by the two methods have already been reported by Baciocchi.[8] However, the nitrate radical efficiency in producing the cation radicals of these precursors is 0.97, much higher than when SET to the $BP^{\bullet+}$ is involved (especially with substrates more difficult to oxidize than **1a**, such as **1d**, **1i**, **1e**, and **1f**), and it is this which has facilitated a detailed investigation of their reactivity.

This difference in efficiency between the present method and other systems, such as DCA/BP/oxygen, is a consequence of the rate of the back-electron-transfer process. For the nitrate radical (E_{ox} = 2.0 V vs SCE) and the 4-methoxybenzyl substrates considered (E_{ox} < 1.70 V vs SCE), back electron transfer between nitrate anion and the benzyl radical cations is endergonic by at least 0.3 eV (Table 3). This suggests a back-electron-transfer rate constant of ca. 10^4−10^5 M^{-1} s^{-1}, too slow to be competitive with unimolecular reactions of the radical cations. Indeed, $\mathbf{1j}^{\bullet+}$, for which no favorable unimolecular fragmentation path is available, decays with a second-order rate constant of this magnitude. It undergoes little irreversible decomposition in preparative experiments, consistent with the suggestion that back electron transfer is the only significant path (Scheme 3).

Cation Radical Fragmentation. In contrast, the other cation radicals undergo fragmentation processes (involving C−H,

(26) (a) Martin, T. W.; Glass, R. W. *J. Am. Chem. Soc.* **1970**, *92*, 5075. (b) Martin, T. W.; Glass, R. W. *J. Am. Chem. Soc.* **1970**, *92*, 5084. (c) Neta, P.; Huie, R. E. *J. Phys. Chem.* **1986**, *90*, 4644. (d) Baciocchi E.; Rol, C.; Sebastiani, G. V.; Serena, B. *Tetrahedron Lett.* **1984**, *1945*. (e) Baciocchi, E.; Del Giacco, E.; Rol, C.; Sebastiani, G. *Tetrahedron Lett.* **1985**, 541.

(27) Baciocchi, E.; Del Giacco, E.; Murgia, M.; Sebastiani, G. *J. Chem. Soc., Chem. Commun.* **1987**, 1246.

(28) Ito, O.; Akiho, S.; Iino, M. *J. Org. Chem.* **1989**, *54*, 2436.

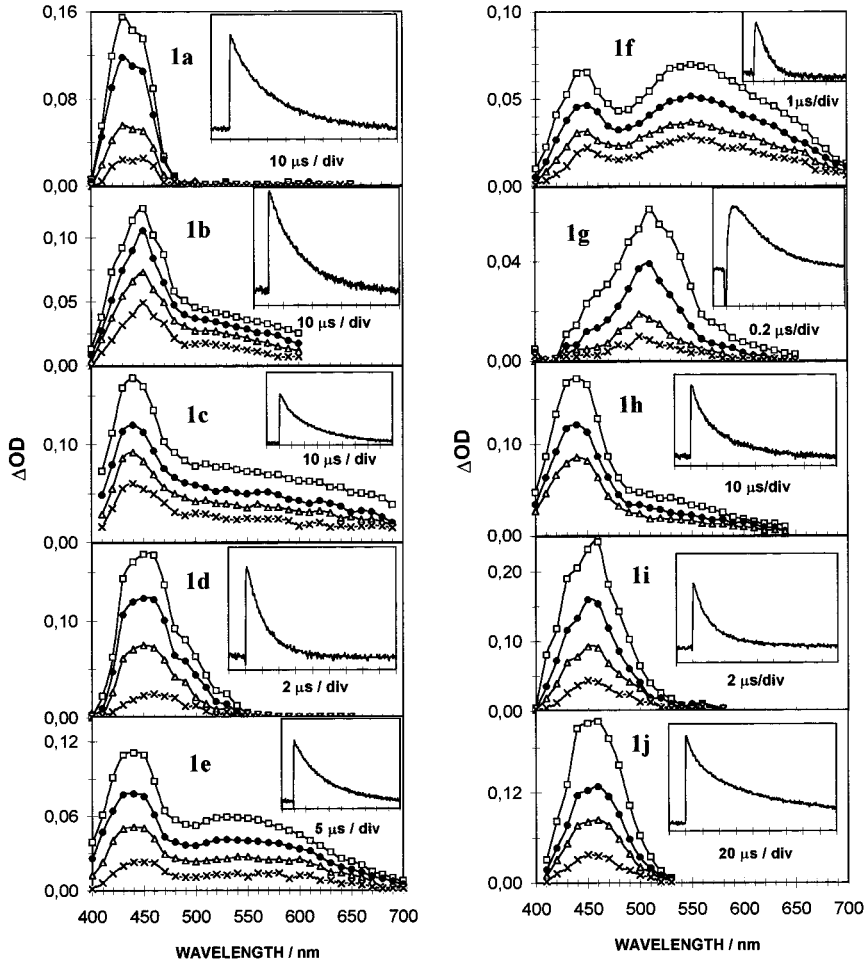

Figure 1. (a) Transient absorption spectra following 355 nm excitation of 5 mM **1a** and 0.5 mM CAN in acetonitrile recorded 1, 5, 20, and 40 μs after the laser pulse. Inset: decay curve for the cation radical recorded at 430 nm. (b) Transient absorption spectra following 355 nm excitation of 5 mM **1b** and 0.5 mM CAN in acetonitrile recorded 1, 2, 10, and 20 μs after the laser pulse. Inset: decay curve for the cation radical recorded at 450 nm. (c) Transient absorption spectra following 355 nm excitation of 5 mM **1c** and 0.5 mM CAN in acetonitrile recorded 1, 5, 10, and 20 μs after the laser pulse. Inset: decay curve for the cation radical recorded at 450 nm. (d) Transient absorption spectra following 355 nm excitation of 5 mM **1d** and 0.5 mM CAN in acetonitrile recorded 0.2, 0.5, 1, and 2 μs after the laser pulse. Inset: decay curve for the cation radical recorded at 460 nm. (e) Transient absorption spectra following 355 nm excitation of 5 mM **1e** and 0.5 mM CAN in acetonitrile recorded 1, 5, 10, and 20 μs after the laser pulse. Inset: decay curve for the cation radical recorded at 440 nm. (f) Transient absorption spectra following 355 nm excitation of 5 mM **1f** and 0.5 mM CAN in acetonitrile recorded 0.2, 0.4, 0.6, and 0.8 μs after the laser pulse. Inset: decay curve for the cation radical recorded at 440 nm. (g) Transient absorption spectra following 355 nm excitation of 5 mM **1g** and 0.5 mM CAN in acetonitrile recorded 0.2, 0.4, 0.8, and 1.6 μs after the laser pulse. Inset: decay curve for the cation radical recorded at 510 nm. (h) Transient absorption spectra following 355 nm excitation of 5 mM **1h** and 0.5 mM CAN in acetonitrile recorded 1, 5, and 10 μs after the laser pulse. Inset: decay curve for the cation radical recorded at 450 nm. (i) Transient absorption spectra following 355 nm excitation of 5 mM **1i** and 0.5 mM CAN in acetonitrile recorded 0.2, 1, 2, and 4 μs after the laser pulse. Inset: decay curve for the cation radical recorded at 440 nm. (j) Transient absorption spectra following 355 nm excitation of 5 mM **1j** and 0.5 mM CAN in acetonitrile recorded 1, 20, 50, and 150 μs after the laser pulse. Inset: decay curve for the cation radical recorded at 460 nm.

C−C, or C−Si bonds) to produce a benzylic radical and a cationic fragment (Scheme 1). The cations evolve either by deprotonation or by nucleophile addition to give identified products (acetone and benzophenone from **1b** and **1c**, respectively; 2-hydroxyethyl formate and 2-hydroxyethyl acetate from **1e** and **1f**, respectively; Table 1). The benzylic radical in turn is oxidized to the corresponding cation by excess CAN (a ratio of CAN: benzylic donor = 2:1 was used), and this cation is trapped by nitrate anion, formed by nitrate radical reduction (Scheme 3), to give the observed benzyl nitrates **2** and **4**, or products **3** and **5** resulting from their further oxidation (Scheme 2 and Table 1). If the CAN solution is more dilute (at least by a factor of 10), acetonitrile competes effectively with nitrate anion for capture of the benzylic cation and acetamide **7h** is formed as an additional product. The CAN-induced conversion of alkyl aromatics to aralkyl nitrates has been considered in

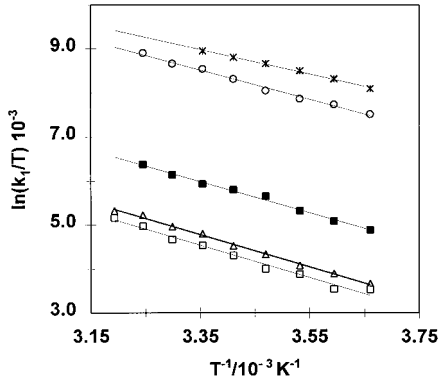

Figure 2. Eyring plot for first-order fragmentation processes in neat acetonitrile, for the following cation radicals: **1b**$^{\bullet+}$ (triangles), **1c**$^{\bullet+}$ (squares), **1e**$^{\bullet+}$ (black squares), **1f**$^{\bullet+}$ (circles), and **1g**$^{\bullet+}$ (stars).

Table 5. Kinetic and Activation Data for the Fragmentation Processes for **1a**$^{\bullet+}$, **1b**$^{\bullet+}$, **1c**$^{\bullet+}$, **1d**$^{\bullet+}$, **1e**$^{\bullet+}$, **1f**$^{\bullet+}$, **1g**$^{\bullet+}$, **1h**$^{\bullet+}$, and **1i**$^{\bullet+}$

(a) Unimolecular Fragmentation Process for **1b**$^{\bullet+}$, **1c**$^{\bullet+}$, **1e**$^{\bullet+}$, **1f**$^{\bullet+}$, and **1g**$^{\bullet+}$ in Acetonitrile

radical cations **1**$^{\bullet+}$	X	fragmentation process[a]	k_1 (10^4 s^{-1}) at 298 K	$\Delta H^{\ddagger}$ [b,c]	$\Delta S^{\ddagger}$ [c,d]	$\Delta G^{\ddagger}$ [b] (298 K)
b	CMe_2OMe	C−C	3.6	+31	−55	+47
c	CPh_2OMe	C−C	2.8	+32	−52	+48
e	1,3-dioxolan-2-yl	C−C	8.5	+29	−40	+45
f	2-methyl-1,3-dioxolan-2-yl	C−C	152.8	+28	−34	+38
g	$SiMe_3$	C−Si	215.0	+23	−46	+37

(b) Bimolecular Fragmentation Process for **1a**$^{\bullet+}$, **1d**$^{\bullet+}$, **1h**$^{\bullet+}$, and **1i**$^{\bullet+}$ Induced by CAN in Acetonitrile

radical cations **1**$^{\bullet+}$	X	fragmentation process[a]	k_2[e] (10^8 M^{-1} s^{-1}) at 298 K	$\Delta H^{\ddagger}$ [b,f]	$\Delta S^{\ddagger}$ [d,f]	$\Delta G^{\ddagger}$ [b] (298 K)
a	H	C−H	0.67	+25	−11	+28
d	COOH	C−C	19.0	+28	+27	+20
h	CH_2OMe	C−H	0.77	+19	−31	+28
i	COOMe	C−H	8.8	+20	−7	+22

(c) Bimolecular Fragmentation Process for **1g**$^{\bullet+}$ Induced by Acetonitrile

radical cation	X	fragmentation process[a]	k_{obs} (10^6 s^{-1}) (298 K)	k_2''[g] (10^5 M^{-1} s^{-1}) (298 K)	$\Delta H^{\ddagger}$ [b,h]	$\Delta S^{\ddagger}$ [d,h]	$\Delta G^{\ddagger}$ [b] (298 K)
1g$^{\bullet+}$	$SiMe_3$	C−Si	2.15[i]	5.5[g]	+22	−60	+40

[a] Deduced from product distribution analysis, Table 1. [b] kJ mol^{-1}. [c] From Eyring plots of k_1 measured over the 0−40 °C range. [d] J mol^{-1} K^{-1}. [e] Second-order rate constant obtained from a linear plot of k_{obs} vs CAN concentration. [f] From Eyring plots of k_2 measured over the 0−40 °C range. [g] Second-order rate constant with acetonitrile as nucleophile, from ref 12. [h] From Eyring plots of k_2'' measured over the 0−25 °C range. [i] In good agreement with the value obtained for the same cation radical produced as a free species with the DCA/BP/O_2 system both in the present investigation and by Dinnocenzo, ref 5.

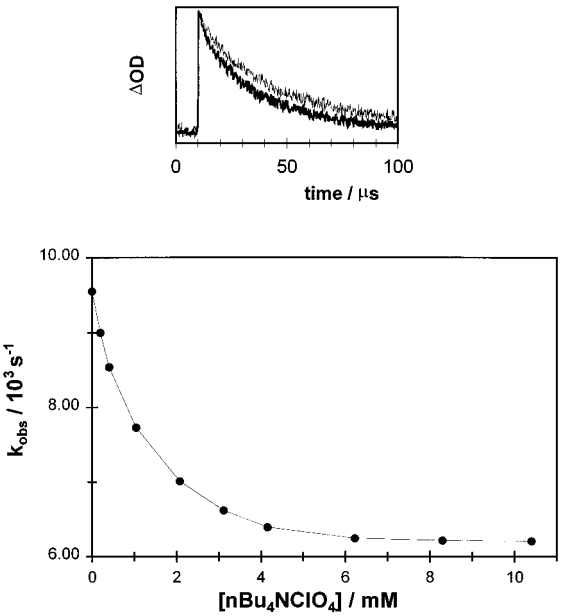

Figure 3. Bottom: Observed rate constant as a function of salt concentration for the decay of **1a**$^{\bullet+}$. Top: Transient absorbance of **1a**$^{\bullet+}$ in the absence and in the presence of salt (0.6 mM, darker line).

detail by Baciocchi and co-workers,[8,10,26d,e,27] and does not require further discussion here.

Product distribution analysis from steady-state photochemical oxidation (Tables 1 and 2) identifies three processes for the cation radicals produced by nitrate radical oxidation. These are (in neat acetonitrile (Table 1)) (a) C−H fragmentation for the radical cations **1a**$^{\bullet+}$, **1h**$^{\bullet+}$, and **1i**$^{\bullet+}$, (b) C−C fragmentation for **1b**$^{\bullet+}$, **1c**$^{\bullet+}$, **1d**$^{\bullet+}$, **1e**$^{\bullet+}$, and **1f**$^{\bullet+}$, and (c) C−Si fragmentation for **1g**$^{\bullet+}$ and (in acetonitrile with added nitrate anion (5 mM) as nucleophile (Table 2)) (a) C−H fragmentation for the radical cations **1a**$^{\bullet+}$, **1b**$^{\bullet+}$, **1c**$^{\bullet+}$, **1e**$^{\bullet+}$, **1h**$^{\bullet+}$, **1i**$^{\bullet+}$, and **1j**$^{\bullet+}$, (b) C−C fragmentation for **1d**$^{\bullet+}$, **1e**$^{\bullet+}$, and **1f**$^{\bullet+}$, and (c) C−Si fragmentation for **1g**$^{\bullet+}$. In every case the material balance was good. The additional product, 2-(4-methoxyphenyl)-1,2-diphenylethanone, obtained from irradiation of **1c,** arose from 1,2-migration of a phenyl group within the cation resulting from the deprotonation of **1c**$^{\bullet+}$ and oxidation of the resulting radical, a process previously observed with similar substrates.[29] There was no significant competitive deprotonation when a C−C or a C−Si benzylic fragmentation occurred, except in the case of cation radical **1e**$^{\bullet+}$ in the presence of added nitrate, when deprotonation and C−C bond fragmentation were both observed. This facilitated interpretation of the fragmentation processes involved in decay of the transients. It is worthwhile to note that the limited salt effect observed on the fragmentation rate is in accordance with the process occurring from the free cation radical. A much larger effect would be expected were an in-cage process involved, due to the strong dependence of the rate of radical ion pair separation on ionic strength.[30]

Decay Kinetics. All cation radicals undergoing C−C or C−Si bond fragmentation underwent first-order decay in acetonitrile, with no dependence on the CAN concentration (k_1, Table 5a). Desilylation of **1g**$^{\bullet+}$, when produced by the CAN method, occurs at the same rate as when using the DCA/BP/O_2 method, as shown both here and in the literature.[5] Since there is literature evidence that this is a solvent-assisted process in acetonitrile,[5] the corresponding k_2'' is reported in Table 5c. In the case of the cation radicals undergoing deprotonation, on the other hand, a CAN-assisted process is involved, and the corresponding rate constant k_2 is reported in Table 5b. Radical cation **1d**$^{\bullet+}$, for which the end result is C−C bond fragmentation, is included in this group, but the primary process is in all likelihood O−H deprotonation (eq 2). In neat acetonitrile the

$$AnCH_2COOH^{\bullet+} \rightarrow AnCH_2COO^{\bullet} \rightarrow AnCH_2^{\bullet} + CO_2 \quad (2)$$

rate constants for the radical cation decays spanned more than

(29) McCall, M. J.; Townsend, J. M.; Bonner, W. A. *J. Am. Chem. Soc.* **1975**, *97*, 2743.
(30) Mattay, J.; Vondenhof, M. *Top. Curr. Chem.* **1991**, *159*, 219.

Table 6. Kinetic and Activation Data for Fragmentation Processes Induced by Nitrate Anion in Acetonitrile

radical cation **1**$^{\bullet+}$	X	fragmentation processes	k_2' [a] (10^8 M^{-1} s^{-1})	$\Delta H^{\ddagger}$ [b,c]	$\Delta S^{\ddagger}$ [c,d]	$\Delta G^{\ddagger}$ [b] (298 K)
a	H	C−H	4.0	+16	−26	+24
h	CH_2OMe	C−H	4.8	+14	−31	+23
b	CMe_2OMe	C−H	2.6	+20	−18	+25
c	CPh_2OMe	C−H	3.2	+19	−21	+25
i	COOMe	C−H	7.1	+14	−27	+22
e	1,3-dioxolan-2-yl	C−H and C−C	4.9	*e*	*e*	*e*
f	2-methyl-1,3-dioxolan-2-yl	C−C	4.4	+20	−12	+24
d	COOH	C−C	13.6	+22	+3	+21
g	$SiMe_3$	C−Si	8.2	+6	−55	+23
j	CMe_3	C−H	0.4			

[a] Second-order rate constant obtained from the plot of k_{obs} vs nitrate concentration at 20 °C. [b] kJ mol^{-1}. [c] From Eyring plots of k_2' measured over the 0−30 °C range. [d] J mol^{-1} K^{-1}. [e] Curved Eyring plot in the 0−30 °C temperature range, consistent with competitive deprotonation and C−C fragmentation for **1e**$^{\bullet+}$ and with the observed product distribution changes; see Table 2.

Table 7. Electrofugacity Scale

radical cations 4-$AnCH_2X^{\bullet+}$	electrofugal group X^+	electrofugacity scale[a]
1a	H^+	1.0 (0.3)[b]
1c	$[CPh_2OMe]^+$	2.8
1b	$[CMe_2OMe]^+$	3.6
1e	[1,3-dioxolan-2-yl]$^+$	8.5
1d	$CO_2 + H^+$	28.3
1f	[2-methyl-1,3-dioxolan-2-yl]$^+$	152.8
1g	$[SiMe_3]^+$	215.0

[a] From the ratios of the (pseudo)-first-order fragmentation rate constants (Table 4) measured in acetonitrile in the presence of CAN (0.15 mM). [b] Value statistically corrected for the number of α-hydrogen atoms.

2 orders of magnitude (Table 4), whereas all transients decayed at a similar rate in the presence of 5 mM nitrate anion (Table 6). Since the rate was much higher than in neat acetonitrile, the second-order rate constant for nitrate-assisted deprotonation, k_2', was directly calculated (Table 6) from k_{obs} and nitrate concentration. In the case of **1f** and **1g** the process remained C−C and C−Si bond fragmentation, respectively, but the decay involved two components (eq 3), since k_1 was not negligible in

$$k_{obs} = k_1 + k_2'[NO_3^-] \quad (3)$$

this case; the k_2' values are reported in Table 6. In the case of **1e** both C−C fragmentation (to give **2** + **3**) and C−H fragmentation (to give **4e**) occurred competitively (Table 2). A curved Eyring plot was obtained over the 0−30 °C temperature range, and kinetic parameters could not be obtained.

Electrofugacity Scale. A large fraction of the radical cations considered cleave in neat acetonitrile to give the same radical, viz., the 4-methoxybenzyl radical. The measured rate constants therefore permit direct comparison between different cationic fragments X^+ as electrofugal groups, and establishment of the electrofugacity scale presented in Table 7. This scale confirms the deductions by Mariano et al.,[6a] from product distribution analysis in the photolysis of *p*-xylene derivatives in the presence of 1,4-dicyanonaphthalene, that $k_{desilylation} > 10k_{decarboxylation} > 10k_{deprotonation}$. Table 7 shows that stabilized α-oxy-substituted carbocations are reasonable electrofugal groups from cation radicals. In particular, the 2-methyl-1,3-dioxolan-2-yl cation is an excellent electrofugal group, its formation being ca. 10 times faster than decarboxylation, where the first step is O−H deprotonation. Its electrofugacity is similar to that of the well-known electrofugal trimethylsilyl cation (pseudo-first-order fragmentation rate constant in acetonitrile at 298 K, 1.53×10^6 and 2.15×10^6 s^{-1}, respectively; Table 5a).

Selectivity of the Fragmentation: Thermochemical Predictions. During the past decade, there have been many publications in the area of radical cation fragmentation and there have been several attempts to find a simple and general approach to the prediction and rationalization of such processes, in particular by intramolecular selectivity involving competition between deprotonation and a different cleavage, as in the present case (Scheme 2). As mentioned earlier, these rationalizations were generally based on comparison of bond dissociation energies (ΔH) in the cation radicals, obtained from thermochemical cycles.[1e,13−15] This approach suffers from the limitation that the entropic contribution cannot be taken into account.

The match between thermochemical prediction and experiment is not always satisfactory. For example, in the intensively studied case of the bibenzyl radical cation in acetonitrile, deprotonation was calculated to be exothermic (ΔH = ca. −60 kJ mol^{-1}) and C−C fragmentation endothermic (ΔH = ca. +40 kJ mol^{-1}), and indeed only the former process is observed.[1g,13−15] As might be anticipated, C−C bond cleavage competes more effectively with C−H bond fragmentation when it leads to a more stable species, and Arnold et al. have shown that in the photooxidation of 1,1,2,2-tetraphenylethane and related systems it is C−C cleavage which occurs.[13−15] However, the lack of deprotonation (in the absence of an added nucleophile) is at first sight surprising, since in these cases also thermochemical calculations indicate that this process is still favored thermodynamically (ΔH_{C-H} significantly negative), even though ΔH_{C-C} is close to zero or only slightly positive. Detailed studies, by the same authors, of the cleavage of bibenzyl derivatives as a function of temperature, have shown that C−C bond fragmentation is the process observed, provided the calculated ΔH is below a threshold of 40−60 kJ mol^{-1}.[15]

There is no clear-cut rationalization for the failure of the thermochemical approach in predicting intramolecular selectivity. Different factors may operate against C−H bond cleavage while favoring competitive C−C or C−Si fragmentations. The most common is the stereoelectronic effect proposed by Baciocchi[20] for α-substituted *p*-xylene radical cations, by Tolbert[11] for 9,10-dialkylanthracene radical cations and by Lewis[2] for deprotonation rates in tertiary amine cation radicals. This suggests that the cleaving β-bond should be collinear with the π-system,[20] though this is generally not the case for the C−H bonds in the most stable conformation(s) of α-substituted benzyl derivatives. However, some objections have been raised to this proposal, mainly by Wagner,[31] and Baciocchi[32] has recently shown that no stereoelectronic effect operates in the cleavage

(31) Wagner, P. J.; Truman, R. J.; Puchalsky, A. E.; Ware, R. *J. Am. Chem. Soc.* **1986**, *108*, 7727.

(32) Baciocchi, E.; Bernini, R.; Lanzalunga, O. *J. Chem. Soc., Chem. Commun.* **1993**, 1691.

Table 8. Thermochemical Cycle Data for Unimolecular Fragmentation Processes of Cation Radicals

$^{\bullet+}$ArCH(H)—X **1**$^{\bullet+}$	X	fragmentation processes (C−Y bond cleavage, Y = α-H or X)	Δ*H*(C−Y) (kJ mol^{-1})	Δ*H*(C−Y$^{\bullet+}$)[a] (kJ mol^{-1})
a	H	C−H	364[b]	23[b]
h	CH_2OMe	C−H	353[c]	8
i	COOMe	C−H	339[d]	−12
b	CMe_2OMe	C−C	272[e]	116[f]
c	CPh_2OMe	C−C	239[g]	72[h]
e	1,3-dioxolan-2-yl	C−C	284[i]	45[j]
f	2-methyl-1,3-dioxolan-2-yl	C−C	272[i]	14[k]
d	COOH	C−C	285[l]	60[m]
g	$SiMe_3$	C−Si	314[n]	140[n]

[a] Estimated on the basis of thermochemical cycles using the equation ΔH (C−Y$^{\bullet+}$) = ΔH(C−Y) + 96.53[$E°$(Y$^{\bullet}$/Y^{+}) − $E°$(ArCH$_2$X)], where ΔH(C−Y$^{\bullet+}$) is the enthalpy (kJ mol^{-1}) for cleavage of the C−Y (Y = α-H or X) bond in the cation radical, ΔH(C−Y) is the enthalpy (kJ mol^{-1}) for cleavage of the same bond in the neutral molecule, $E°$(ArCH$_2$X) is the oxidation potential in V vs SCE of the neutral benzylic donor (from Table 3), and $E°$(Y$^{\bullet}$/Y^{+}) is the reduction potential of the electrofugal group. For Y = H, $E°$(H$^{\bullet}$/H^{+}) = −2.01V vs SCE (= −1.77V vs NHE, ref 54) has been used. For other Y substituents, values from refs 55 and 56 were used. [b] Data from ref 8. [c] Assuming the same value as for 4-MeOC$_6$H$_4$**C**HMe−**H**, ref 8. [d] Assuming the same value as for 4-MeOC$_6$H$_4$**C**H(CN)−**H,** ref 8. [e] From ref 57. [f] The oxidation potential of the radical Me$_2$C$^{\bullet}$−OMe was assumed to be the same as that of Me$_2$C$^{\bullet}$-OCHMe$_2$, −0.10 V, ref 56. [g] Estimated from ΔH for Ph**C**H$_2$−**C**HPh$_2$, ref 15. [h] Estimating an oxidation potential for Ph$_2$C$^{\bullet}$−OMe of −0.23 V from that for PhCH$^{\bullet}$−OMe (−0.33V) in ref 55. [i] Estimated values from ref 57. [j] Using an oxidation potential for the 1,3-dioxolan-2-yl radical of −0.88 V (−0.90 V vs Ag/AgCl) from ref 58. [k] Using an oxidation potential for the 2-methyl-1,3-dioxolan-2-yl radical of −1.13 V (−1.15 vs Ag/AgCl) from ref 58. [l] Assuming the same ΔH as for Ph**C**H$_2$−**C**OOH from ref 57. [m] Using an oxidation potential for the couple HOOC$^{\bullet}$/CO$_2$ + H^{+} of −0.65 V from ref 59. [n] From gas-phase data in ref 5.

of a benzylic carbon−silicon bond in a conformationally fixed aromatic cation radical.

These considerations show the limited value of the thermochemical approach in predicting and rationalizing the reactivity of radical cations, especially when deprotonation competes with other bond fragmentation processes. Part of the problem may arise from the exclusion of the entropic factor. A more severe limitation, however, arises from a lack of some of the redox data required when applying thermochemical cycles. In particular, these are available only for a few carbocations, and are not available for silyl cations. In those cases, estimates or approximations have to be made when applying gas phase parameters to reactions in solution, and obviously such predictions are subject to large errors.

Application of the thermochemical approach to the presently considered 4-methoxybenzyl radical cations **1**$^{\bullet+}$ leads to the values listed in Table 8, using the approximation previously adopted by Arnold,[15] i.e., that ΔS(4-MeOC$_6$H$_4$CH$_2$X) = ΔS(4-MeOC$_6$H$_4$CH$_2$X$^{\bullet+}$). These fail to correctly rationalize both the intramolecular selectivity and the relative reactivity of different substrates. Thus, while the ΔH(C−H$^{\bullet+}$) values are quite low, the ΔH(C−C$^{\bullet+}$) values are in general higher (Table 8), and in some cases above the previously mentioned limit proposed by Arnold. The ΔH(C−Si$^{\bullet+}$) value is still higher, though the value thus calculated is not directly comparable since it refers to gas-phase fragmentation (Table 8). Nevertheless, as seen above, C−C and C−Si bond fragmentations do occur in the cases indicated in Table 5, although with all substrates ΔH(C−H$^{\bullet+}$) is estimated to be lower than ΔH(C−X$^{\bullet+}$), due to $E°$(H$^{\bullet}$/H^{+}) being so much more negative than $E°$(X$^{\bullet}$/X^{+}) (see footnotes to Table 8).

Fragmentation Selectivity: Activation Parameters. The present study of the decay kinetics of cation radicals as a function of temperature allows the activation parameters to be calculated and provides the appropriate base for discussing these fragmentation processes in solution. This approach has been used before by Dinnocenzo[7] and Parker[18] independently to describe the bimolecular deprotonation process induced by bases (pyridines, quinuclidines, and acetate) in tertiary amine cation radicals using stopped flow and electrochemical techniques, respectively. Maslak applied the same approach to C−C unimolecular fragmentation processes in the cation radicals of bicumyls.[16] Very recently Schanze[19a] and co-workers measured energies of activation for bond fragmentations in the radical cations of amino alcohols, a system extensively studied by Whitten,[1p,19b] but in these cases only C−C fragmentation was observed. Our study is the first attempt to apply a single experimental approach to comparison of C−H, C−C, and C−Si bond fragmentation processes in radical cations.

For the radical cations undergoing deprotonation in neat acetonitrile (**1a**$^{\bullet+}$, **1h**$^{\bullet+}$, **1i**$^{\bullet+}$), the fragmentation occurs via a second-order process involving assistance by the cerium complex through an as yet unspecified mechanism. At any rate, the present finding, together with previous literature evidence,[7−9] supports a general rule, viz., that radical cations obtained from easily oxidizable substrates [and thus having a positive, if small, ΔH(C−H$^{\bullet+}$)] undergo deprotonation at a carbon center only in the presence of an added base. The activation parameters listed in Table 5a refer to this bimolecular fragmentation process. Deprotonations involving the cation radicals **1a**$^{\bullet+}$, **1h**$^{\bullet+}$, and **1i**$^{\bullet+}$ have negative $\Delta S^{\ddagger}$ values, similar to the situation found for the activation entropies measured by Dinnocenzo for tertiary amine radical cation bimolecular deprotonation induced by quinuclidine.[7] Likewise, Parker reported even more negative $\Delta S^{\ddagger}$ values in the deprotonation of *N*,*N*-dimethylanilines using pyridine as base.[18] The corresponding $\Delta H^{\ddagger}$ values for the CAN-assisted process are positive (19−28 kJ mol^{-1}) and in the same range reported by Parker and Dinnocenzo for deprotonation of tertiary amine cation radicals. However, closer direct comparison of the data is inappropriate in view of the differences in the systems used in the two cases. As might be anticipated, there is a general trend for the activation enthalpy values (Table 5b) to fall in line with the BDEs of the neutral molecule (Table 8) while the activation entropy values (Table 5b) are strongly affected by both steric (compare **1a**$^{\bullet+}$ with **1h**$^{\bullet+}$) and electronic factors (compare **1h**$^{\bullet+}$ with **1i**$^{\bullet+}$).

Cation radical **1d**$^{\bullet+}$ should be considered separately. Here the overall process involves C−C fragmentation, but the process observed by flash photolysis is deprotonation from the oxygen atom followed by, or more likely concerted with, C−C fragmentation. Thus, it is not surprising that its activation parameters largely differ from those of the other cation radicals (Table 5b) that are acidic at carbon. The positive value of $\Delta S^{\ddagger}$ for **1d**$^{\bullet+}$ is consistent with the fact that it fragments with

production of a third fragment (CO_2). These different values for the activation parameters for **1d**$^{\bullet+}$ fragmentation, with higher $\Delta H^{\ddagger}$ and more positive $\Delta S^{\ddagger}$, are also observed in the bimolecular process induced by nitrate anion (Table 6).

For the radical cations undergoing C−C (**1b**$^{\bullet+}$, **1c**$^{\bullet+}$, **1e**$^{\bullet+}$, **1f**$^{\bullet+}$) or C−Si (**1g**$^{\bullet+}$) bond fragmentation a first-order process occurs (Table 5a). The temperature-dependent kinetic data reveal that this fragmentation is characterized by very low activation enthalpies [lower than expected from the calculated ΔH(C−C$^{\bullet+}$) values (Table 8), though these suffer from a significant error] and negative activation entropies (Table 5a), a trend similar to that found by Maslak[16b,c] and Schanze[19a] for bicumyl and amino alcohol radical cations, respectively.

In their studies of a series of bibenzyl derivatives with similar electrofugal groups, Arnold et al.[15] had previously found a threshold value for ΔH of 35−42 kJ mol^{-1} for the C−C bond fragmentation process on the basis of a thermochemical approach which considered the entropic terms to be negligible. In the present case, activation parameters rather than thermochemical values are directly measured and a range of electrofugal groups is considered. The results demonstrate that the activation entropic term plays a key role in controlling the value of $\Delta G^{\ddagger}$. Comparison of the activation parameters (Table 5a) for **1b**$^{\bullet+}$ (electrofugal group: CMe_2OMe^+) and **1f**$^{\bullet+}$ (electrofugal group: the 2-methyl-1,3-dioxolan-2-yl cation) shows that the $\Delta H^{\ddagger}$ term is very similar for both (ca. 10% difference), whereas the $\Delta S^{\ddagger}$ term for **1b**$^{\bullet+}$ is more negative by ca. 40% than that for **1f**$^{\bullet+}$. It is therefore more the entropic term which determines the larger value of $\Delta G^{\ddagger}$ at 25 °C for **1b**$^{\bullet+}$ than for **1f**$^{\bullet+}$, and which results in C−C bond fragmentation being more favored for the latter radical cation. Indeed, in the case of **1f**$^{\bullet+}$ first-order C−C bond fragmentation remains competitive with second-order C−C fragmentation in the presence of 5 mM nitrate, whereas with **1b**$^{\bullet+}$ second-order deprotonation completely dominates. Similar conclusions may be drawn from a comparison of the activation parameters for **1c**$^{\bullet+}$ and **1f**$^{\bullet+}$ (Table 5a).

In the case of **1g**$^{\bullet+}$ desilylation is the only process which occurs. Since Dinnocenzo and co-workers have shown that this process is assisted by acetonitrile, activation parameters were calculated in this case for bimolecular fragmentation involving the solvent, and the resulting values are in excellent agreement[12c] with theirs (in their case **1g**$^{\bullet+}$ was produced by PET to DCA). The $\Delta H^{\ddagger}$ for the C−Si fragmentation process is the lowest of the series, much lower than the ΔH value calculated for the gas phase (125 kJ mol^{-1}) by Dinnocenzo and showing that correct application of the thermochemical approach requires appropriate input data; indeed, the limitations of applying gas-phase data to solution-phase evaluation are apparent from the above comparison. The $\Delta S^{\ddagger}$ value is strongly negative (−60 J K^{-1} mol^{-1}, Table 5c).

Fragmentation Selectivity: Effect of the Nucleophile. In the presence of a more effective nucleophile than the solvent acetonitrile, all the radical cations undergo second-order decay, nitrate anion being used because of its compatibility with CAN. Deprotonation is observed for radical cations **1a**$^{\bullet+}$, **1b**$^{\bullet+}$, **1c**$^{\bullet+}$, **1e**$^{\bullet+}$, **1h**$^{\bullet+}$, **1i**$^{\bullet+}$, and **1j**$^{\bullet+}$ while C−C fragmentation occurs for **1e**$^{\bullet+}$ and **1f**$^{\bullet+}$, and C−Si fragmentation for **1g**$^{\bullet+}$. These observations again support the suggestion that deprotonation requires, at least with these substrates, a better base than acetonitrile, e.g., CAN or nitrate anion. More importantly, they show that when the nucleophilicity of the system is slightly increased by the addition of nitrate, radical cations which have $\Delta G^{\ddagger}$ higher than +45 kJ mol^{-1} in the absence of nitrate (**1b**$^{\bullet+}$, **1c**$^{\bullet+}$, **1e**$^{\bullet+}$; Table 5a) change their fragmentation process from C−C bond cleavage to deprotonation, suggesting that this is the limit for competition between C−C and C−H fragmentation.

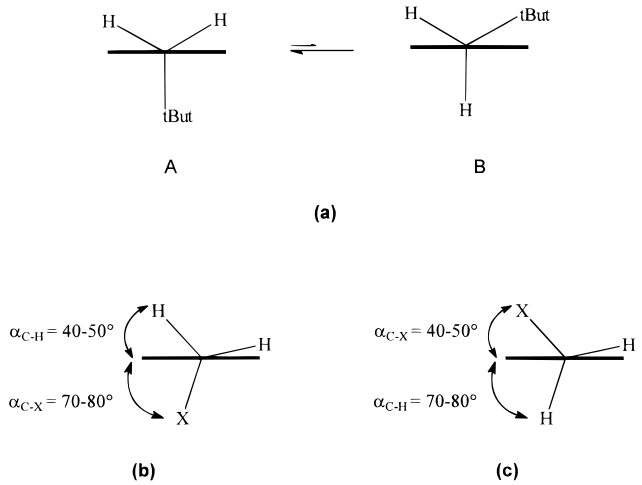

Figure 4. (a) Conformations populated by **1j**$^{\bullet+}$. (b) "Folded"conformation, populated by **1f**$^{\bullet+}$ and, to a much lesser extent, by **1e**$^{\bullet+}$. (c) "Stretched" conformation, populated by **1b**$^{\bullet+}$, **1c**$^{\bullet+}$, and **1h**$^{\bullet+}$.

For the nitrate-induced process, all the radical cations studied fragment via a second-order process, although in the case of **1g**$^{\bullet+}$ and **1f**$^{\bullet+}$ a significant first-order component remains. The k_2' values and the related activation parameters are listed in Table 6. The data permit a homogeneous comparison of the C−H, C−C, and C−Si fragmentation processes on the basis of these activation parameters, the first such comparison in the literature to date. All the cation radicals are associated with very similar free energy changes during fragmentation (22−25 kJ mol^{-1}). The $\Delta H^{\ddagger}$ contributions for deprotonation are all slightly below 20 kJ mol^{-1}, while those for C−C bond fragmentation are marginally above that value, though the differences are small. On the other hand, the scatter of $\Delta S^{\ddagger}$ contributions is more marked, with somewhat more negative values observed for deprotonation (−18 to −31 J mol^{-1} K^{-1}) than for C−C fragmentation (−12 J mol^{-1} K^{-1} for **1f**$^{\bullet+}$). This outcome suggests that competition between C−H and C−C fragmentation is temperature dependent, as verified in the case of **1e**$^{\bullet+}$ which indeed shows a temperature-dependent product distribution. Nucleophile-assisted fragmentation of **1d**$^{\bullet+}$, with O−H deprotonation as the key step (eq 2), again shows a positive $\Delta S^{\ddagger}$, although smaller than in neat acetonitrile. Desilylation is characterized by a very low $\Delta H^{\ddagger}$.

Deprotonation. Different rates for α-deprotonation in benzylic radical cations have previously been explained on the basis of the steric influence of the α-substituent. A preferred conformation involving effective overlap of the C−H bond with the aromatic π-system would be most suitable for cleavage, and it has been suggested that substituents which hinder the achievement of this conformation result in decreased rates of deprotonation (stereoelectronic effect).[10,20]

Among the present substrates, such a classical steric effect is apparent in the slower (by a factor of 10) deprotonation rate of **1j**$^{\bullet+}$ as compared to **1a**$^{\bullet+}$. AM1 calculations, using the half electron approximation,[55] show two significant conformers (Figure 4a). Conformer A, more stable than conformer B by 10 kJ mol^{-1}, has the *tert*-butyl group oriented so as to minimize unfavorable steric interactions with the aromatic ring. As a consequence the orientation of the benzylic C−H bonds precludes favorable overlap with the aromatic π-system, and a much slower rate of deprotonation is observed relative to **1a**$^{\bullet+}$, for which favorable overlap can occur.

On the other hand the deprotonation rates for **1b**$^{\bullet+}$, **1c**$^{\bullet+}$, and **1h**$^{\bullet+}$ are very similar despite the different steric demands of their α-substituents. This suggests the operation of a different conformational effect, for which we have some supporting evidence. Thus, some of the cation radicals show (Figure 1) a long wavelength absorption tail (**1b**$^{\bullet+}$, **1c**$^{\bullet+}$, and **1h**$^{\bullet+}$) or a separate maximum (**1e**$^{\bullet+}$ and **1f**$^{\bullet+}$). This suggests an intramolecular interaction with charge-transfer (CT) character which might, in combination with the steric effect, be influential in determining the preferred conformational outcome. Preliminary AM1 calculations support the existence of two groups of conformational minima. In the "folded" conformation (Figure 4b), the β-substituent is partially superimposed on the π-cloud, with a distance of 2.7−2.9 Å between the oxygen of the β-substituent and the closer sp^2 carbon atom, and a less-than-favorable torsion angle between the benzylic C−H bond and the aromatic ring of approximately 40−50°. In the "stretched" conformation (Figure 4c) the β-substituent is much further from the aromatic ring and results in a much more favorable torsion angle between the benzylic C−H bond and the aromatic ring of 70−80°.

The stretched conformations are more stable, by more than 8.5 kJ mol^{-1}, than the folded ones for **1b**$^{\bullet+}$, **1c**$^{\bullet+}$, and **1h**$^{\bullet+}$, thereby also facilitating benzylic C−H bond cleavage. It is this favorable alignment of the benzylic C−H bond with the aromatic π-system for **1a**$^{\bullet+}$, **1b**$^{\bullet+}$, **1c**$^{\bullet+}$, and **1h**$^{\bullet+}$ which may account for the similarities in their nitrate-induced deprotonation rates.

The importance of the stabilizing intramolecular CT effect in influencing the conformational equilibrium is even greater for β,β-dioxy-substituted radical cations, for which the folded conformation becomes more important. In the cases of **1e**$^{\bullet+}$ and **1f**$^{\bullet+}$, the energy difference between the more stable stretched conformation and the less stable folded conformation reduces to 5.0 and 0.8 kJ mol^{-1}, respectively.

Carbon−Carbon and Carbon−Silicon Bond Fragmentations vs Deprotonation. There has been no previously reported evidence for related bimolecular carbon−carbon bond fragmentations. In particular, Maslak has extensively studied such fragmentations in tetrasubstituted bibenzyl cation radicals, and has consistently found *unimolecular* processes occurring with relatively low rates.[16] The fastest reaction in his case is for 1,1,2,2-tetrabutyl-1-(4′-(dimethylamino)phenyl)-2-phenylethane radical cation ($k_1 = 5.4 \times 10^5$ s^{-1}) in which a highly sterically hindered weak bond is cleaved to give a stabilized cation and a stabilized radical. In contrast, the present radical cations are much more energetic (by ca. 0.9 eV) and undergo cleavage of a much stronger bond. It is therefore not surprising that in this case a fast ($k_2 = 4.4 \times 10^8$ M^{-1} s^{-1} for **1f**$^{\bullet+}$) *bimolecular* reaction with a nucleophile occurs, considering also that a less hindered center is involved.

In attempting to rationalize the factors which determine which of the possible fragmentation pathways is followed, calculations of the charge density at the β-carbon were undertaken. It might be anticipated that the nitrate anion would be sensitive to its magnitude at the reacting center, and indeed an interesting trend was observed. Computational analysis shows that the charge density was low for **1j**$^{\bullet+}$ (−0.04) and for **1b**$^{\bullet+}$, **1c**$^{\bullet+}$, and **1h**$^{\bullet+}$ (about −0.02) but higher for **1e**$^{\bullet+}$ (+0.16) and **1f**$^{\bullet+}$ (+0.22), and reaching a maximum for **1g**$^{\bullet+}$ (+1.2). On the other hand the charge density on the benzylic hydrogens remains almost constant for all these radical cations, with no dependence on the substituent and only a limited dependence on the dihedral angle, remaining in the range +0.12 to +0.16 as the dihedral angle between the plane of the aromatic ring and the benzylic C−H bond was increased from 30° to close to 90°. This may explain the preference for attack at *carbon* in **1f**$^{\bullet+}$ and at *silicon* in **1g**$^{\bullet+}$, for which the charge density at the β-center in both is greater than at the benzylic hydrogens, and at the benzylic *hydrogens* for **1b**$^{\bullet+}$, **1c**$^{\bullet+}$, **1h**$^{\bullet+}$, and **1j**$^{\bullet+}$, for which the benzylic hydrogens have the higher charge. For **1e**$^{\bullet+}$ both processes compete and the appropriate charge densities were found to be practically identical.

Mechanism of Nitrate-Assisted Fragmentation Processes. The present processes are fast, though by no means diffusion-controlled.[17c] With the exception of carboxylic acid **1d**$^{\bullet+}$, where O−H deprotonation occurs, and **1j**$^{\bullet+}$, where C−H deprotonation is 10 times slower than for **1a**$^{\bullet+}$, the second-order rate constants span a remarkably narrow range[33a] (2.6×10^8 to 8.2×10^8 M^{-1} s^{-1}). This is despite the fact that the various processes observed involve nitrate interaction with such different H, C, and Si electrophilic centers in the different radical cations **1**$^{\bullet+}$. Thus, the rates for benzylic carbon−hydrogen bond cleavage (**1a**$^{\bullet+}$), carbon−carbon bond cleavage (**1f**$^{\bullet+}$), and carbon−silicon bond cleavage (**1g**$^{\bullet+}$) are remarkably similar (Table 6). Transfer of an electrofugal group to nitrate anion, a *hard* nucleophile, is therefore only slightly influenced by the structure of the group being transferred.[33b]

The remarkable similarities in the rates of bond cleavage for **1a**$^{\bullet+}$, **1f**$^{\bullet+}$, and **1g**$^{\bullet+}$ are suggestive of a process whose rate-determining step is essentially independent of the nature of the bond which is subsequently broken. They are consistent with an early transition state[33c] in which formation of the activated complex occurs largely without involvement of the fragmenting bond and any differences between these bonds become kinetically insignificant as cleavage occurs later along the reaction coordinate. The observation that the transient absorption spectra of the radical cations remain unchanged in the presence of nitrate eliminates the possibility that the rate similarities might be due to the rate-determining formation of a nitrate/radical cation intermediate.

A more detailed analysis shows that the entropic term ($\Delta S^{\ddagger}$) contributes more in the carbon−carbon bond fragmentations than in the deprotonations, while the enthalpic term ($\Delta H^{\ddagger}$) contributes more to the deprotonations than to the carbon−carbon cleavages. This suggests a model for the transition-state complex in these processes. When the nucleophile acts as a base, the interaction (with the proton) is stronger ($\Delta H^{\ddagger}$ is lower) and requires a higher degree of organization in the transition state; i.e., the activation complex is "tighter" ($\Delta S^{\ddagger}$ is more negative). On the other hand, when the nucleophile interacts with a different electrofugal group, such as a carbocation, the interaction is weaker ($\Delta H^{\ddagger}$ is higher) and the transition state is looser ($\Delta S^{\ddagger}$ is less negative), resembling more the cation radical precursors. Importantly, in this sense the silyl cation resembles more the proton than a carbocation.

Conclusions

The investigation described above has demonstrated that laser spectroscopic techniques can be used for the generation and kinetic characterization of ion radical intermediates. Detailed study of competing fragmentation processes in 4-methoxybenzyl

(33) (a) Deprotonation rates of the same magnitude have been reported[8] by Baciocchi et al. for related substrates. (b) This is not the case for softer nucleophiles. For example, in the desilylation of **1g**$^{\bullet+}$, the rate increases by over 3 orders of magnitude (from 5.5×10^5 to 8.2×10^8 M^{-1} s^{-1}) as the nucleophile is changed from acetonitrile[12a] to nitrate anion (Table 6). (c) Baciocchi et al. have also reported[10] the involvement of early transition states with related substrates.

derivatives has provided detailed mechanistic information about cation radical fragmentation.

(1) An electrofugacity scale (in acetonitrile) based on direct fragmentation rate measurements has been established, confirming the previously indirect prediction that C−Si and C−C bond fragmentation can compete with deprotonation.

(2) Activation parameters for C−H, C−C, and C−Si bond fragmentations have been measured. The observed trend of $\Delta H^{\ddagger}$ values roughly parallels those obtained from thermochemical cycles (at least when the latter are based upon reliable redox data) and suggests that enthalpic factors contribute more to deprotonation than to C−C bond fragmentation in radical cations. On the other hand, the trend of the observed $\Delta S^{\ddagger}$ values and the differences between such values for the C−C and C−H fragmentation processes points to the importance of the entropic contribution in determining the course of fragmentation processes in cation radicals.

(3) Evidence for direct transfer of both silicon and carbon electrofugal groups to a weak nucleophile such as nitrate anion has been obtained.

(4) The operation of both electronic and steric effects in determining the conformation of the radical cation (and thus its reactivity) has been evidenced and supported by calculation.

Previous direct measurements have been carried out with more stabilized cation radicals, such as the aromatic amines studied by Saveant[17] and the aminobicumyls studied by Maslak.[16] In the present study, more energetic species have been chosen and their fragmentation modes have been determined in the presence both of weak (acetonitrile) and of strong (nitrate anion) nucleophiles. Further extension of the conclusions to yet more energetic species such as the cation radicals formed from poorer donors exemplified by benzyl derivatives lacking the methoxy substituent, where thermochemically calculated ΔH values are often strongly negative, may require some care. However, it is unlikely that similar direct measurements can be made for such species, and some extrapolation of the presently observed trends is reasonable. Important predictions include the conditions under which C−Si and C−C fragmentation paths are competitive with deprotonation, and the medium effect on the selectivity. Coupled with the possibility of generating cation radicals even from poor donors under mild conditions, particularly through photoinduced SET, such knowledge should increase interest in these fragmentations as an unconventional method for generating radicals and ions for synthetic purposes.

Experimental Section

General Procedures. NMR spectra were recorded in $CDCl_3$ solutions on a Bruker AC400 spectrometer, and chemical shifts are reported in parts per million relative to Me_4Si as internal standard. IR spectra were recorded using a Perkin-Elmer System 2000 FT-IR spectrometer and are reported in wavenumbers (cm^{-1}) for liquids as films on NaCl plates or for solids as dispersions in KBr. Product distribution in the presence of added nitrate was determined by GC, using a HP 5890 instrument, column HP-5 (5% phenyl methyl silicone) 10 m × 0.53 mm × 2.65 μm film thickness. Elemental analyses were determined using a Carlo Erba Model 1106 instrument.

Materials. Cerium(IV) ammonium nitrate (Carlo Erba 99.9%) was dried under vacuum (0.01 mmHg) at 40 °C for 1 day. 4-Methoxytoluene (**1a**; Aldrich), (4-methoxyphenyl)acetic acid (**1d**; Aldrich), methyl (4-methoxyphenyl)acetate (**1i**; Aldrich), tetra-*n*-butylammonium nitrate (Aldrich), and tetra-*n*-butylammonium perchlorate (Fluka) were obtained commercially. 2-Methoxy-2-methyl-1-(4-methoxyphenyl)-propane (**1b**),[34] 1,1-diphenyl-1-methoxy-2-(4-methoxyphenyl)ethane (**1c**), and 1-methoxy-2-(4-methoxyphenyl)ethane (**1h**)[35] were prepared by the Williamson reaction from the corresponding alcohols (Aldrich), using a previously reported procedure.[35] 2-(4-Methoxybenzyl)-1,3-dioxolane (**1e**) and 2-methyl-2-(4-methoxybenzyl)-1,3-dioxolane (**1f**)[36] were prepared from ethylene glycol and (4-methoxyphenyl)acetaldehyde[37,38] (using the procedure of ref 36) or (4-methoxyphenyl)acetone (Aldrich) by azeotropic distillation according to a standard procedure.[36] (4-Methoxybenzyl)trimethylsilane (**1g**) was prepared and purified according to a published procedure.[39] 2,2-Dimethyl-1-(4-methoxyphenyl)propane (**1j**)[40] was prepared following a procedure used for the synthesis of neopentylbenzenes.[41]

Preparation of 1,1-Diphenyl-1-methoxy-2-(4-methoxyphenyl)-ethane (1c). 1,1-Diphenyl-2-(4-methoxyphenyl)ethanol was obtained following the procedure of ref 41. Using the procedure described in ref 34 for the alkylation of 2-methoxy-1-(4-methoxyphenyl)ethane (**1h**), the 1,1-diphenyl-2-(4-methoxyphenyl)ethanol[42] (9.0 g, 30 mmol) was methylated with dimethyl sulfate (7.56 g, 60 mmol) to give, after recrystallization from MeOH, 1,1-diphenyl-1-methoxy-2-(4-methoxyphenyl)ethane (**1c**) (7.50 g, 79%) as white crystals: mp 94−95 °C; ^{1}H NMR 3.16 (s, 3H, OCH_3), 3.55 (s, 2H, CH_2), 3.71 (s, 3H, OCH_3), 6.61 and 6.64 (AA′BB′ system, J = 9.0 Hz, 4H, aromatic), 7.19−7.26 (m, 10H, aromatic); ^{13}C NMR 40.5 (CH_2), 50.8 (OCH_3), 55.0 (OCH_3), 83.4 (quaternary), 112.8, 126.7, 127.5, 127.7 and 131.3 (CH, aromatic), 128.7, 144.8 and 157.7 (aromatic, ipso). Anal. Calcd for $C_{22}H_{22}O_2$: C, 82.99; H, 6.96. Found: C, 82.90; H, 6.91.

2-(4-Methoxybenzyl)-1,3-dioxolane (**1e**): colorless liquid (bp 102 °C, 0.02 mmHg); ^{1}H NMR 2.90 (d, J = 4.9 Hz, 2H, benzylic CH_2), 3.77 (s, 3H, OCH_3), 3.80−3.87 (m, 2H, OCH_2), 3.89−3.95 (m, 2H, OCH_2), 5.00 (t, 1H, J = 4.9 Hz, CH), 6.83 and 7.17 (AA′BB′ system, J = 8.4 Hz, 4H, aromatic); ^{13}C NMR 39.8 (CH_2), 55.1 (OCH_3), 64.9 (OCH_2), 104.7 (OCHO), 113.7 and 130.5 (aromatic, CH), 128.1 and 158.2 (aromatic, ipso); IR 3410, 2960, 1605, 1510, 1270, 1080. Anal. Calcd for $C_{11}H_{14}O_3$: C, 68.02; H, 7.27. Found: C, 67.93; H, 7.24.

2-Methyl-2-(4-methoxybenzyl)-1,3-dioxolane (**1f**)**:**[36] colorless liquid (bp 110 °C, 0.02 mmHg); ^{1}H NMR 1.28 (s, 3H, CH_3), 2.85 (s, 2H, benzylic CH_2), 3.71−3.74 (m, 2H, OCH_2), 3.77 (s, 3H, OCH_3), 3.86−3.90 (m, 2H, OCH_2), 6.80 and 7.16 (AA′BB′ system, J = 8.4 Hz, 4H, aromatic); ^{13}C NMR 24.2 (CH_3), 44.4 (CH_2), 55.2 (OCH_3), 64.8 (OCH_2), 109.8 (quaternary), 113.3 and 1313 (aromatic, CH), 129.0 and 158.2 (aromatic, ipso); IR 3405, 2958, 1610, 1500, 1255, 1066.

Photochemical Reactions. General Procedure. An acetonitrile solution (20 mL) of CAN (219 mg, 0.4 mmol) and 4-methoxytoluene (**1a**) (24.4 mg, 0.2 mmol) in a Pyrex tube (25 mL capacity) was deaerated by flushing with nitrogen and then irradiated through a Pyrex filter using a 400 W medium-pressure mercury vapor lamp for 30 min at room temperature. After irradiation the solvent was removed under vacuum at 10 °C. Water (15 mL) and CH_2Cl_2 (15 mL) were added to the solid, and the mixture was shaken thoroughly. The organic layer was washed once with water and then dried over $MgSO_4$. The solvent was removed under vacuum at 0 °C. The resulting mixture was dissolved in $CDCl_3$, adding 1,4-dibromobenzene or 1,4-dinitrobenzene as an internal standard. The ^{1}H and ^{13}C NMR spectra of the crude photoproduct mixture were recorded and the product yields obtained. The product, 4-methoxybenzyl nitrate (**2**), was identified by comparison with an authentic sample.

The other reactions were similarly carried out. Product **5i** was purified by silica gel chromatography (cyclohexane:ethyl acetate = 9:1) and identified by comparison of its physical properties with those

(34) Bunnett, J. F.; Sridharan, S. *J. Org. Chem.* **1979**, *44*, 1458.
(35) Bird, C. W.; Brown, A. L. *Tetrahedron* **1985**, *41*, 4685.
(36) Humphreys, D. J.; Lawrence, P. M.; Newall, C. E.; Phillipps, G. H.; Wall, P. A. *J. Chem. Soc., Perkin Trans. 1* **1978**, 24.
(37) Crotti, P.; Ferretti, M.; Macchia, F.; Stoppioni, A. *J. Org. Chem.* **1986**, *51*, 2759.
(38) Lambert, J. B.; Mark, H. W.; Magyar, E. S. *J. Am. Chem. Soc.* **1977**, *99*, 3059.
(39) Coughlin, D. J.; Salomon, R. G. *J. Org. Chem.* **1979**, *44*, 3784.
(40) Jaxa-Chamiec, A.; Shah, V. P.; Kruse, L. I. *J. Chem. Soc., Perkin Trans. 1* **1989**, 1705.
(41) Bassindale, A. R.; Eaborn, C.; Walton, D. R. M. *J. Chem. Soc. C* **1969**, 2505.
(42) Norman, R. O. C.; Watson, R. A. *J. Chem. Soc. B* **1968**, 692.

reported in the literature.[43] The nitrate **4i** was identified by comparison with an authentic sample synthesized via an alternative pathway, as reported below.

Due to its instability, the nitrate **4h** was not characterized as such but was hydrolyzed to the alcohol **6h**[44] by shaking a solution of the crude photolyzate in ether for a few minutes (at room temperature) with a 5% solution of $NaHCO_3$ in water. 2-Hydroxyethyl formate and 2-hydroxyethyl acetate were identified in the crude photolyzate by comparison of their ^{1}H NMR and ^{13}C NMR spectral data with literature values.[45]

4-Methoxybenzaldehyde (**3**) was identified by comparison with an authentic sample (Aldrich).

The acetamide **7h** was purified by chromatography of the crude photolyzate on silica gel (ethyl acetate:MeOH = 20:1), after eluting the unreacted starting material and the alcohol **6h** (cyclohexane:ethyl acetate = 1:1).

***N*-[2-Methoxy-1-(4-methoxyphenyl)ethyl]acetamide (7h):** yellow solid (mp 110−112 °C, from MeOH); ^{1}H NMR 1.95 (s, 3H, CH_3), 3.25 (s, 3H, OCH_3), 3.57 (d, 2H, J = 4 Hz, OCH_2), 3.69 (s, 3H, OCH_3), 5.0 (dt, 1H, J = 4 Hz, J = 3 Hz), 6.12 (d, 1H, J = 3 Hz, NH), 6.85 and 7.12 (AA′BB′ system, J = 9.0 Hz, 4H, aromatic);^{13}C NMR 23.3 (CH_3), 51.8 (NCH), 55.1 (OCH_3), 58.9 (OCH_3), 74.8 (OCH_2), 113.8, 127.8 (aromatic, CH), 131.9, 158.8 (aromatic, ipso), 169.4 (CO); IR 3339 (sharp), 3050, 1642, 1515, 1251, 1181, 1125, 1085, 1027, 825. Anal. Calcd for $C_{12}H_{17}NO_3$: C, 64.55; H, 7.67; N, 6.27. Found: C, 64.44; H, 7.60; N, 6.32.

4-Methoxybenzyl Nitrate (2). This material was obtained in quantitative yield following a published procedure.[46] A stoichiometric amount of 4-methoxybenzyl chloride was added to a solution of $AgNO_3$ in acetonitrile. The mixture was stirred for 10 min, AgCl was filtered off, and the solvent was removed. The residue was a colorless oil which decomposed at T > 90 °C: ^{1}H NMR 3.80 (s, 3H, OCH_3), 5.35 (s, 2H, CH_2ONO_2), 6.89 and 7.31 (AA′BB′ system, J = 9.0 Hz, 4H, aromatic); ^{13}C NMR 55.3 (OCH_3), 74.9 (CH_2), 114.2 and 131.1 (aromatic, CH), 124.0 and 160.6 (aromatic, ipso); IR 2962, 2840, 2553, 1628, 1516, 1280, 1253, 860. Anal. Calcd for $C_8H_9NO_4$: C, 52.46; H, 4.95; N, 7.65. Found: C, 52.35; H, 4.91; N, 7.59.

α-Carbomethoxy-4-methoxybenzyl Nitrate (4i). Methyl 4-methoxymandelate,[47] prepared from 4-methoxymandelic acid following a standard esterification procedure,[48] was obtained in quantitative yield as a colorless liquid: bp 100−102 °C, 0.05 mmHg [lit.[47] mp 32−34 °C, lit.[48] bp(8 mmHg) 162 °C]; ^{1}H NMR 3.39 (s, 1H, OH), 3.74 (s, 3H, OCH_3), 3.79 (s, 3H, OCH_3), 5.11 (s, 1H, CH), 6.87 and 7.30 (AA′BB′ system, J = 8.9 Hz, 4H, aromatic); ^{13}C NMR 52.9 (OCH_3), 55.2 (OCH_3), 72.4 (CH), 114.0 and 127.8 (aromatic, CH), 130.4 and 159.7 (aromatic, ipso), 174.3 (C═O); IR 3443 (br), 2967, 2841, 1728, 1611, 1512, 1215, 1180.

On the basis of a published synthesis of ethyl 2-(chlorophenyl)-acetate,[49] methyl 2-(4-methoxyphenyl)-2-chloroacetate was synthesized from methyl 4-methoxymandelate. To a stirred CH_2Cl_2 solution (25 mL) of methyl 4-methoxymandelate (1.7 g, 8.67 mmol) was added dropwise a CH_2Cl_2 solution (25 mL) of $SOCl_2$ (0.7 mL, 9 mmol) over 10 min. The solution was heated under reflux for 2 h and then cooled to room temperature, and water (10 mL) was added. After the solution was stirred for 20 min, the organic layer was washed three times with water and dried. Removal of the solvent under vacuum gave methyl 2-(4-methoxyphenyl)-2-chloroacetate (1.45 g, 78%) as a colorless liquid: bp 85−89 °C, 0.05 mmHg; ^{1}H NMR 3.75 (s, 3H, OCH_3), 3.79 (s, 3H, OCH_3), 5.32 (s, 1H, CH), 6.87 and 7.39 (AA′BB′ system, J = 8.9 Hz, 4H, aromatic); ^{13}C NMR 53.2 (OCH_3), 55.3 (OCH_3), 58.7 (CH), 114.2 and 129.3 (aromatic, CH), 127.7 and 160.3 (aromatic, ipso), 169.0 (C═O); IR 2956, 2839, 1754, 1611, 1513, 1304, 1255, 1163. Anal. Calcd for $C_{10}H_{11}ClO_3$: C, 55.96; H, 5.17. Found: C, 55.85; H, 5.15.

Following the procedure described above for **2**, methyl 2-(4-methoxyphenyl)-2-chloroacetate was converted quantitatively to α-carbomethoxy-(4-methoxybenzyl)nitrate (**4i**) by reaction with $AgNO_3$ in acetonitrile: ^{1}H NMR 3.76 (s, 3H, OCH_3), 3.79 (s, 3H, OCH_3), 5.99 (s, 1H, CH), 6.90 and 7.33 (AA′BB′ system, J = 8.9 Hz, 4H, aromatic); ^{13}C NMR 52.9 (OCH_3), 55.3 (OCH_3), 81.3 (CH), 114.5 and 130.0 (aromatic, CH), 121.2 and 161.2 (aromatic, ipso), 167.8 (C═O); IR 2960, 2843, 2560, 1755, 1642, 1611, 1516, 1293, 1257, 1178. Anal. Calcd for $C_{10}H_{11}NO_6$: C, 49.80; H, 4.59; N, 5.81. Found: C, 49.70; H, 4.50; N, 5.82.

Photochemical Reactions in the Presence of Tetrabutylammonium Nitrate. General Procedure. An acetonitrile solution (300 mL) of CAN (329 mg, 2 mM), **1b** (60 mg, 1 mM), and *n*-Bu_4NNO_3 (460 mg, 5 mM) was deaerated by flushing with nitrogen and then irradiated for 30 min at room temperature in a water-cooled immersion well using a 125 W medium-pressure mercury vapor lamp fitted with a Pyrex filter. After the irradiation, water (50 mL) was added and the solution was stirred for 1 h. Removal of the solvent under vacuum at room temperature yielded a solid. Diethyl ether (50 mL) was added, the mixture was shaken thoroughly, and the organic layer was washed twice with water and dried over $MgSO_4$. Nitrate **4b** contained in the mixture was hydrolyzed by shaking a solution in ether with a 5% solution of $NaHCO_3$ in water. The product **6b** was purified by silica gel column chromatography using cyclohexane−ethyl acetate (4:1) as eluent.

The other reactions were similarly carried out, and the products **6c, 6e**,[50] **6h**,[44] and 1-(4-methoxyphenyl)-1,2-diphenylethanone[51] were similarly isolated.

Reaction in the case of **1j** was slow, and only part conversion was achieved. Nitrate **4j** was identified in the crude reaction mixture, after workup as described above, by ^{1}H NMR: 1.05 (s, 9H, tBu), 3.84 (s, 3H, OCH_3), 5.40 (s, 1H), 6.90 and 7.26 (AA′BB′ system, J = 9.0 Hz, 4H, aromatic).

2-Methoxy-1-(4-methoxyphenyl)-2-methylpropan-1-ol (6b): colorless oil; ^{1}H NMR 1.03 (s, 3H, CH_3), 1.10 (s, 3H, CH_3), 3.05 (br s, 1H, OH), 3.3 (s, 3H, OCH_3), 3.80 (s, 3H, OCH_3), 4.55 (s, 1H, CH benzylic), 6.85 and 7.30 (AA′BB′ system, J = 9.0 Hz, 4H, aromatic); ^{13}C NMR 18.1 (CH_3), 20.9 (CH_3), 49.4 (OCH_3), 55.1 (OCH_3), 78.1 (C−OMe), 78.7 (benzylic CH), 112.9 and 128.7 (aromatic, CH), 132.0 and 158.9 (aromatic, ipso); IR 3500, 2977, 2837, 1612, 1585, 1248, 1069, 817. Anal. Calcd for $C_{12}H_{18}O_3$: C, 68.54; H, 8.63. Found: C, 68.42; H, 8.51.

2-Methoxy-1-(4-methoxyphenyl)-2,2-diphenylethanol (6c): colorless oil; ^{1}H NMR 2.65 (br s, 1H, OH), 3.05 (s, 3H, OCH_3), 3.75 (s, 3H, OCH_3), 5.60 (s,1H, benzylic H), 6.60 and 6.70 (AA′BB′ system, J = 9.0 Hz, 4H, aromatic), 7.15−7.35 (m, 10H, aromatic); ^{13}C NMR 50.5 (OCH_3), 54.8 (OCH_3), 76.9 (benzylic CH), 83.2 (C quaternary), 113.0, 126.6, 127.3, 127.6 and 130.3 (aromatic, CH), 130.7, 144.8 and 158.7 (aromatic, ipso). Anal. Calcd for $C_{22}H_{22}O_3$: C, 79.02; H, 6.63. Found: C, 78.89; H, 6.60.

2-Methoxy-1-(4-methoxyphenyl)ethanol (6h):[44] colorless liquid; ^{1}H NMR 2.70 (br s, 1H, OH), 3.40 (dd, J = 3 Hz, J = 8 Hz, 1H), 3.45 (s, 3H, OCH_3), 3.52 (dd, J = 3 Hz, J = 8 Hz, 1H), 3.79 (s, 3H, OCH_3), 4.82 (dd, J = 8 Hz, 1H), 6.85 and 7.27 (AA′BB′ system, J = 9.0 Hz, 4H, aromatic) (in agreement with the ^{1}H NMR spectrum reported in

(43) Katritzky, A. R.; Wang, Z.; Well, A. P. *Org. Prep. Proced. Int.* **1995**, *27*, 457.
(44) Blumenstein, J. J.; Ukachukwn, V. C.; Mohan, R. S.; Whalen, D. L. *J. Org. Chem.* **1993**, *58*, 924.
(45) Halmo, F.; Materdes, A. *Petrochemia* **1981**, *21*, 121. (b) Barrelle, M.; Beguin, C.; Tessier, S. *Org. Magn. Reson.* **1982**, *19*, 102.
(46) Baciocchi, E.; Rol, C.; Mandolini, L. *J. Org. Chem.* **1977**, *42*, 3682.
(47) Kolasa, T.; Miller, M. *J. Org. Chem.* **1987**, *52*, 4978.
(48) Barthel, W., F.; Leon, J.; Hall, S. A. *J. Org. Chem.* **1954**, *19*, 485.
(49) Eliel, E. L.; Fisk, M. T.; Prosser, T. *Organic Syntheses;* Wiley: New York, 1963; *Collect.* Vol. IV, p 169.
(50) Shiner, C. S.; Tsunoda, T.; Goodman, B. A.; Ingham, S.; Lee, S−H.; Vorndam, P. E. *J. Am. Chem. Soc.* **1989**, *111*, 1381.
(51) Dilgen, S. F.; Hennessy, D. J. *J. Org. Chem.* **1962**, *27*, 1223.
(52) Fukuzumi, S.; Kochi, J. K. *J. Org. Chem.* **1981**, *46*, 4116.
(53) Griller, D.; Simoes, M.; Molder, J. A.; Sim, B. A.; Wayner, D. D. M. *J. Am. Chem. Soc.* **1989**, *111*, 7872.
(54) Wayner, D. D. M.; Parker, V. D. *Acc. Chem. Res.* **1993**, *26*, 287.
(55) Wayner, D. D. M.; Sim, B. A.; Dannenberg, J. J. *J. Org. Chem.* **1991**, *56*, 4853.
(56) Wayner, D. D. M.; McPhee, D. J.; Griller, D. *J. Am. Chem. Soc.* **1988**, *110*, 132.
(57) McMillen, D. F.; Golden, D. M. *Annu. Rev. Phys. Chem.* **1982**, *33*, 493.
(58) Fontana, F.; Kolt, R. J.; Huang, Y.; Wayner, D. D. M. *J. Org. Chem.* **1994**, *59*, 4671.
(59) Papaconstantinous, E. *Anal. Chem.* **1975**, *47*, 1592.

ref 44); ^{13}C NMR 55.2 (OCH_3), 58.9 (OCH_3), 72.1 (CH_2O), 78.1 (benzylic CH), 113.7, 127.3 (aromatic, CH), 132.2 and 159.2 (aromatic, ipso); IR 3440 (br), 3050, 1618, 1515, 1250, 1110, 835.

2-(4-Methoxyphenyl)-1,2-diphenylethanone:[51] pale yellow solid, recrystallized from methanol; mp 87−89 °C (lit.[51] mp 89−90 °C); ^{1}H NMR 3.77 (s, 3H, OCH_3), 5.95 (s, 1H, CH), 6.83 and 7.45 (AA′BB′ system, J = 9.0 Hz, 4H, aromatic), 7.15−7.55 (m, 8H, aromatic), 7.95−8.05 (m, 2H, aromatic); ^{13}C NMR 55.1 (OCH_3), 58.4 (CH), 114.0, 126.9, 128.4, 128.5, 128.8, 128.9, 130.0, 130.9, 132.8, 136.7, 139.3, 158.5 (aromatics), 198.3 (CO); IR 1684. Anal. Calcd for $C_{21}H_{18}O_2$: C, 83.42; H, 6.00. Found: C, 83.34; H, 6.10.

2-Methoxy-1-(4-methoxyphenyl)-2,2-diphenylethanone (5c): pale yellow oil; ^{1}H NMR 3.05 (s, 3H, OCH_3), 3.80 (s, 3H, OCH_3), 6.83 and 8.05 (AA′BB′ system, J = 9.5 Hz, 4H, aromatic), 7.20−7.50 (m, 10H, aromatic); ^{13}C NMR 53.1 (OCH_3), 54.9 (OCH_3), 90.8 (quaternary C), 113.2, 127.8, 128.0, 128.8, 132.1, 140.8, 144.5, 158.6 (aromatics), 203.0 (CO); IR 1672. Anal. Calcd for $C_{22}H_{20}O_3$: C, 79.50; H, 6.06. Found: C, 79.43; H, 5.99.

Laser Flash Photolysis. The laser pulse photolysis apparatus consisted of a Spectron Laser System SL801 Nd:YAG laser used at the third harmonic of its fundamental wavelength. It delivered a maximum power of 30 mJ at 355 nm with 10 ns pulse duration. The monitor system, arranged in a cross-beam configuration, consisted of a 275 W Xe arc lamp, an F/3.4 monochromator, and a five-stage photomultiplier supplied by Applied Photophysics. The signals were captured by a Hewlett-Packard 54510A digitizing oscilloscope, and the data were processed on a 286-based computer system using software developed in-house. Solutions for analysis were placed in a fluorescence cuvette (d = 10 mm). The absorbance of each solution was adjusted to 1.4 with the exception of the measurements of decay rates as a function of CAN concentration, for which the absorbance was between 0.8 and 1.8.

Acknowledgment. Support of this research by the European Union under its Human Capital and Mobility Research Program (Contract No. ERBCHRXCT930151) is gratefully acknowledged.

JA970940S